Méthode de type Galerkin discontinu en maillages multi-éléments pour la résolution numérique des équations de Maxwell instationnaires

Clément Durochat

Équipe-projet NACHOS, INRIA Sophia Antipolis - Méditerranée, France

Soutenance de thèse, 30 Janvier 2013
Directeur : Stéphane Lanteri

Étude soutenue par la Région Île-de-France dans le cadre du projet MIEL3D-MESHER du cluster Systematic Paris-Région

Outline

Outline

- Mathematical model to describe the propagation of electromagnetic waves
- Synthesis of existing experimental laws $\Longrightarrow$ unification and improvement by James Clerk Maxwell :

$$\begin{cases} \partial_t \mathbf{B} + \mathrm{curl}(\mathbf{E}) = 0 & : \text{Maxwell-Faraday equations} \\ \partial_t \mathbf{D} - \mathrm{curl}(\mathbf{H}) + \mathbf{j} = 0 & : \text{Maxwell-Ampère equations} \\ \mathrm{div}(\mathbf{D}) = \rho & : \text{Maxwell-Gauss equation} \\ \mathrm{div}(\mathbf{B}) = 0 & : \text{Magnetic flux equation} \end{cases}$$

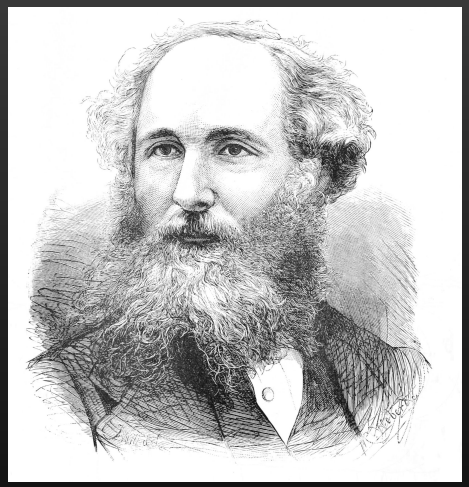

James Clerk Maxwell (13 June 1831 – 5 November 1879)

- We consider linear, isotropic and non-dispersive media

- Mathematical model to describe the propagation of electromagnetic waves
- Synthesis of existing experimental laws $\Longrightarrow$ unification and improvement by James Clerk Maxwell :

$$\begin{cases} \partial_t \mathbf{B} + \mathrm{curl}(\mathbf{E}) = 0 & : \text{Maxwell-Faraday equations} \\ \partial_t \mathbf{D} - \mathrm{curl}(\mathbf{H}) + \mathbf{j} = 0 & : \text{Maxwell-Ampère equations} \\ \mathrm{div}(\mathbf{D}) = \rho & : \text{Maxwell-Gauss equation} \\ \mathrm{div}(\mathbf{B}) = 0 & : \text{Magnetic flux equation} \end{cases}$$

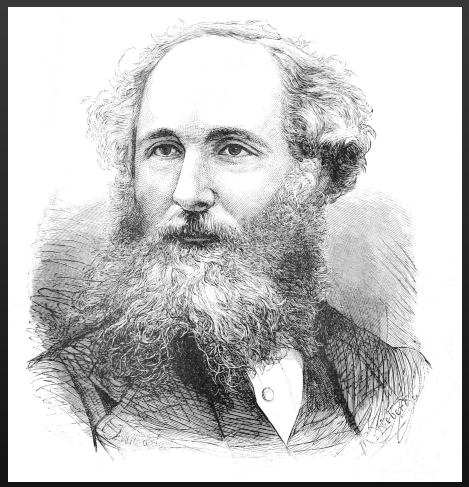

James Clerk Maxwell (13 June 1831 – 5 November 1879)

- We consider linear, isotropic and non-dispersive media

Ω, bounded polyhedral domain of $\mathbb{R}^3$, boundary $\Gamma = \Gamma^a \cup \Gamma^m$;
the system of Maxwell equations in three space dimensions is given by :

$$\left\{ \begin{array}{rcl} \varepsilon \partial_t \mathbf{E} - \mathrm{curl}(\mathbf{H}) & = & -\sigma \mathbf{E} - \mathbf{j_s}, \\ \mu \partial_t \mathbf{H} + \mathrm{curl}(\mathbf{E}) & = & 0, \end{array} \right.$$

where :

- $\mathbf{E} \equiv (E_1(\mathbf{x}, t), E_2(\mathbf{x}, t), E_3(\mathbf{x}, t))^{\mathrm{T}}$ & $\mathbf{H} \equiv (H_1(\mathbf{x}, t), H_2(\mathbf{x}, t), H_3(\mathbf{x}, t))^{\mathrm{T}}$ are the electric field and the magnetic field
- $\varepsilon \equiv \varepsilon(\mathbf{x})$, $\mu \equiv \mu(\mathbf{x})$, are the electric permittivity and the magnetic permeability, respectively
- $\sigma \equiv \sigma(\mathbf{x})$, $\mathbf{j_s} \equiv \mathbf{j_s}(\mathbf{x}, t)$, are the electric conductivity and a current source, respectively
- Metallic boundary condition on Γ^m : $\mathbf{n} \times \mathbf{E} = 0$ ($\mathbf{n}$ outwards normal to Γ)

  Silver-Müller boundary condition on Γ^a : $\mathbf{n} \times \mathbf{E} - \sqrt{\frac{\mu}{\varepsilon}} \mathbf{n} \times (\mathbf{H} \times \mathbf{n}) = 0$

Ω, bounded polyhedral domain of $\mathbb{R}^3$, boundary $\Gamma = \Gamma^a \cup \Gamma^m$;
the system of Maxwell equations in three space dimensions is given by :

$$\left\{ \begin{array}{rcl} \varepsilon \partial_t \mathbf{E} - \mathrm{curl}(\mathbf{H}) & = & -\sigma \mathbf{E} - \mathbf{j_s}, \\ \mu \partial_t \mathbf{H} + \mathrm{curl}(\mathbf{E}) & = & 0, \end{array} \right.$$

where :

- $\mathbf{E} \equiv (E_1(\mathbf{x}, t), E_2(\mathbf{x}, t), E_3(\mathbf{x}, t))^{\mathrm{T}}$ & $\mathbf{H} \equiv (H_1(\mathbf{x}, t), H_2(\mathbf{x}, t), H_3(\mathbf{x}, t))^{\mathrm{T}}$ are the electric field and the magnetic field
- $\varepsilon \equiv \varepsilon(\mathbf{x})$, $\mu \equiv \mu(\mathbf{x})$, are the electric permittivity and the magnetic permeability, respectively
- $\sigma \equiv \sigma(\mathbf{x})$, $\mathbf{j_s} \equiv \mathbf{j_s}(\mathbf{x}, t)$, are the electric conductivity and a current source, respectively
- Metallic boundary condition on Γ^m : $\mathbf{n} \times \mathbf{E} = 0$ ($\mathbf{n}$ outwards normal to Γ)
  Silver-Müller boundary condition on Γ^a : $\mathbf{n} \times \mathbf{E} - \sqrt{\frac{\mu}{\varepsilon}} \mathbf{n} \times (\mathbf{H} \times \mathbf{n}) = 0$

- Finite Difference Time-Domain method (FDTD)

[1] K. S. Yee. *Numerical solution of initial boundary value problems involving Maxwell's equations in isotropic media.* IEEE Trans. on. Antennas and Propag., vol. 14, pp. 302–307, 1966.

[2] A. Taflove and S. C. Hagness. *Computational electrodynamics : the finite-difference time-domain method - 3rd ed.* Artech House Publishers, 2005.

- Finite Element Time-Domain method (FETD)

[3] J.-C. Nedelec. *Mixed finite elements in* $\mathbb{R}^3$. Numer. Math., vol. 35, pp. 315–341, 1980.

[4] S. Pernet, X. Ferrieres and G. Cohen. *High spatial order finite element method to solve Maxwell's equations in time domain* IEEE Trans. on Antennas and Propag., vol. 53, no. 9, pp. 2889–2899, 2006.

- Finite Volume Time-Domain method (FVTD)

[5] S. Piperno, M. Remaki and L. Fezoui. *A nondiffusive finite volume scheme for the three-dimensional Maxwell's equations on unstructured meshes.* SIAM J. Numer. Anal., vol. 39, no. 6, pp. 2089–2108, 2002.

- Discontinuous Galerkin Time-Domain method (DGTD, "GD" in french)

[6] F. Bourdel, P.A. Mazet and P. Helluy. *Resolution of the non-stationary or harmonic Maxwell equations by a discontinuous finite element method. Application to an E.M.I. (electromagnetic impulse) case* In proc. of 10th Inter. Conf. on Comp. Meth. in Appl. Sc. and Eng., pp. 1–18, 1992.

[7] J. S. Hesthaven and T. Warburton. *Nodal high-order methods on unstructured grids. I. Time-domain solution of Maxwell's equations.* J. Comput. Phys., vol. 181, no. 1, pp. 186–221, 2002.

[8] B. Cockburn, F. Li and C.-W. Shu. *Locally divergence-free discontinuous Galerkin methods for the Maxwell equations.* J. Comput. Phys., vol. 194, pp. 588–610, 2004.

[9] G. Cohen, X. Ferrieres and S. Pernet. *A spatial high order hexahedral discontinuous Galerkin method to solve Maxwell's equations in time-domains.* J. Comput. Phys., vol. 217, no. 2, pp. 340–363, 2006.

Outline

- FDTD with FVTD, or with FETD, or with DGTD

[10] X. Ferrieres, J.-P. Parmantier, S. Bertuol and A. R. Ruddle. *Application of a hybrid finite difference/finite volume method to solve an automotive EMC problem.* IEEE Trans. on Eletromag. Compatibility, vol. 46, no. 4, pp. 624–634, 2004.

[11] L. Beilina and M. J. Grote. *Adaptive hybrid finite element/difference method for Maxwell's equations.* STWMS J. Pure Appl. Math., vol. 1, no. 2, pp. 176–197, 2010.

[12] S. G. Garcia, M. F. Pantoja, C. M. de Jong van Coevorden, A. R. Bretones and R. G. Martin. *A new hybrid DGTD/FDTD method in 2-D.* IEEE Microw. Wireless Compon. Lett., vol. 18, no. 12, pp. 764–766, 2008.

- Spectral FETD with DGTD

[13] R.W. Davies, K. Morgan and O. Hassan. *A high order hybrid finite element method applied to the solution of electromagnetic wave scattering problems in the time domain* Comput. Mech., vol. 44, pp. 321–331, 2009.

- 2D DGTD on hybrid meshes for seismic waves

[14] V. Hermann, M. Käser and C. E. Castro. *Non-conforming hybrid meshes for efficient 2-D wave propagation using the Discontinuous Galerkin Method.* Geophys. J. Int., vol. 184, pp. 746–758, 2010.

Objective : Formulate, validate, and study a DGTD-$\mathbb{P}_p\mathbb{Q}_k$ method to solve Maxwell equations :

- mesh objects with complex geometry by tetrahedra (triangles in 2D) for high precision
- mesh the surrounding space by square elements (large size) for simplicity and speed

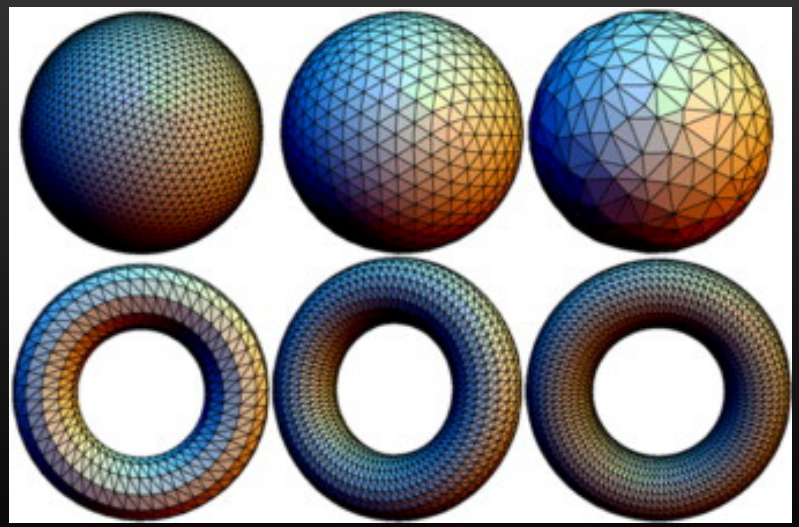

- Pseudo-conservative form ($\mathbf{W} = (\mathbf{E}, \mathbf{H})^{\mathrm{T}} \in \mathbb{R}^6$) : $Q(\partial_t \mathbf{W}) + \nabla \cdot F(\mathbf{W}) = \mathbf{J}$
- Ω is discretized by $\mathscr{C}_h = \bigcup_{i=1}^{N} c_i = \mathscr{T}_h \bigcup \mathscr{Q}_h$, where c_i are tetrahedra ($\in \mathscr{T}_h$) or hexahedra ($\in \mathscr{Q}_h$) in 3D (triangles or quadrangles in 2D)
- For theoretical aspects we consider $\mathbf{J} \equiv 0$ and only metallic boundaries
- We denote by $\vec{\psi} = (\psi_1, \psi_2, \psi_3, \psi_4, \psi_5, \psi_6)^{\mathrm{T}} \in \mathbb{R}^6$ a vector test function. By dot multiplying (Euclidean, designated by $\langle . \ , \ . \rangle$) the pseudo-conservative form with $\vec{\psi}$ and integrating on c_i, we have a first weak form :

$$\int_{c_i} \langle Q(\partial_t \mathbf{W}) \ , \ \vec{\psi} \rangle d\mathbf{x} + \int_{c_i} \langle \nabla \cdot F(\mathbf{W}) \ , \ \vec{\psi} \rangle d\mathbf{x} = 0$$

- $\mathbb{P}_p[c_i]$: space of polynomial functions with degree at most p on $c_i \in \mathscr{T}_h$ (form of polynomials $\mathbb{P}_1$ in 2D : $\beta_0 + \beta_1 x_1 + \beta_2 x_2$), with local basis $\phi_i = (\varphi_{i1}, \varphi_{i2}, \ldots, \varphi_{id_i})$
- $\mathbb{Q}_k[c_i]$: space of polynomial functions with degree at most k with respect to each variable separately on $c_i \in \mathscr{Q}_h$ (form of polynomials $\mathbb{Q}_1$ in 2D : $\gamma_0 + \gamma_1 x_1 + \gamma_2 x_2 + \gamma_3 x_1 x_2$), with local basis $\theta_i = (\vartheta_{i1}, \vartheta_{i2}, \ldots, \vartheta_{ib_i})$

- Pseudo-conservative form ($\mathbf{W} = (\mathbf{E}, \mathbf{H})^{\mathrm{T}} \in \mathbb{R}^6$) : $Q(\partial_t \mathbf{W}) + \nabla \cdot F(\mathbf{W}) = \mathbf{J}$
- Ω is discretized by $\mathscr{C}_h = \bigcup_{i=1}^{N} c_i = \mathscr{T}_h \bigcup \mathscr{Q}_h$, where c_i are tetrahedra ($\in \mathscr{T}_h$) or hexahedra ($\in \mathscr{Q}_h$) in 3D (triangles or quadrangles in 2D)
- For theoretical aspects we consider $\mathbf{J} \equiv 0$ and only metallic boundaries
- We denote by $\vec{\psi} = (\psi_1, \psi_2, \psi_3, \psi_4, \psi_5, \psi_6)^{\mathrm{T}} \in \mathbb{R}^6$ a vector test function. By dot multiplying (Euclidean, designated by $\langle . \ , \ . \rangle$) the pseudo-conservative form with $\vec{\psi}$ and integrating on c_i, we have a first weak form :

$$\int_{c_i} \left\langle Q(\partial_t \mathbf{W}) \ , \ \vec{\psi} \right\rangle d\mathbf{x} + \int_{c_i} \left\langle \nabla \cdot F(\mathbf{W}) \ , \ \vec{\psi} \right\rangle d\mathbf{x} = 0$$

- $\mathbb{P}_p[c_i]$: space of polynomial functions with degree at most p on $c_i \in \mathscr{T}_h$ (form of polynomials $\mathbb{P}_1$ in 2D : $\beta_0 + \beta_1 x_1 + \beta_2 x_2$), with local basis $\phi_i = (\varphi_{i1}, \varphi_{i2}, \ldots, \varphi_{id_i})$
- $\mathbb{Q}_k[c_i]$: space of polynomial functions with degree at most k with respect to each variable separately on $c_i \in \mathscr{Q}_h$ (form of polynomials $\mathbb{Q}_1$ in 2D : $\gamma_0 + \gamma_1 x_1 + \gamma_2 x_2 + \gamma_3 x_1 x_2$), with local basis $\theta_i = (\vartheta_{i1}, \vartheta_{i2}, \ldots, \vartheta_{ib_i})$

- Pseudo-conservative form ($\mathbf{W} = (\mathbf{E}, \mathbf{H})^{\mathrm{T}} \in \mathbb{R}^6$) : $Q(\partial_t \mathbf{W}) + \nabla \cdot F(\mathbf{W}) = \mathbf{J}$
- Ω is discretized by $\mathscr{C}_h = \bigcup_{i=1}^{N} c_i = \mathscr{T}_h \bigcup \mathscr{Q}_h$, where c_i are tetrahedra ($\in \mathscr{T}_h$) or hexahedra ($\in \mathscr{Q}_h$) in 3D (triangles or quadrangles in 2D)
- For theoretical aspects we consider $\mathbf{J} \equiv 0$ and only metallic boundaries
- We denote by $\vec{\psi} = (\psi_1, \psi_2, \psi_3, \psi_4, \psi_5, \psi_6)^{\mathrm{T}} \in \mathbb{R}^6$ a vector test function. By dot multiplying (Euclidean, designated by $\langle . \ , \ . \rangle$) the pseudo-conservative form with $\vec{\psi}$ and integrating on c_i, we have a first weak form :

$$\int_{c_i} \left\langle Q(\partial_t \mathbf{W}) \ , \ \vec{\psi} \right\rangle d\mathbf{x} + \int_{c_i} \left\langle \nabla \cdot F(\mathbf{W}) \ , \ \vec{\psi} \right\rangle d\mathbf{x} = 0$$

- $\mathbb{P}_p[c_i]$: space of polynomial functions with degree at most p on $c_i \in \mathscr{T}_h$ (form of polynomials $\mathbb{P}_1$ in 2D : $\beta_0 + \beta_1 x_1 + \beta_2 x_2$), with local basis $\phi_i = (\varphi_{i1}, \varphi_{i2}, \ldots, \varphi_{id_i})$
- $\mathbb{Q}_k[c_i]$: space of polynomial functions with degree at most k with respect to each variable separately on $c_i \in \mathscr{Q}_h$ (form of polynomials $\mathbb{Q}_1$ in 2D : $\gamma_0 + \gamma_1 x_1 + \gamma_2 x_2 + \gamma_3 x_1 x_2$), with local basis $\theta_i = (\vartheta_{i1}, \vartheta_{i2}, \ldots, \vartheta_{ib_i})$

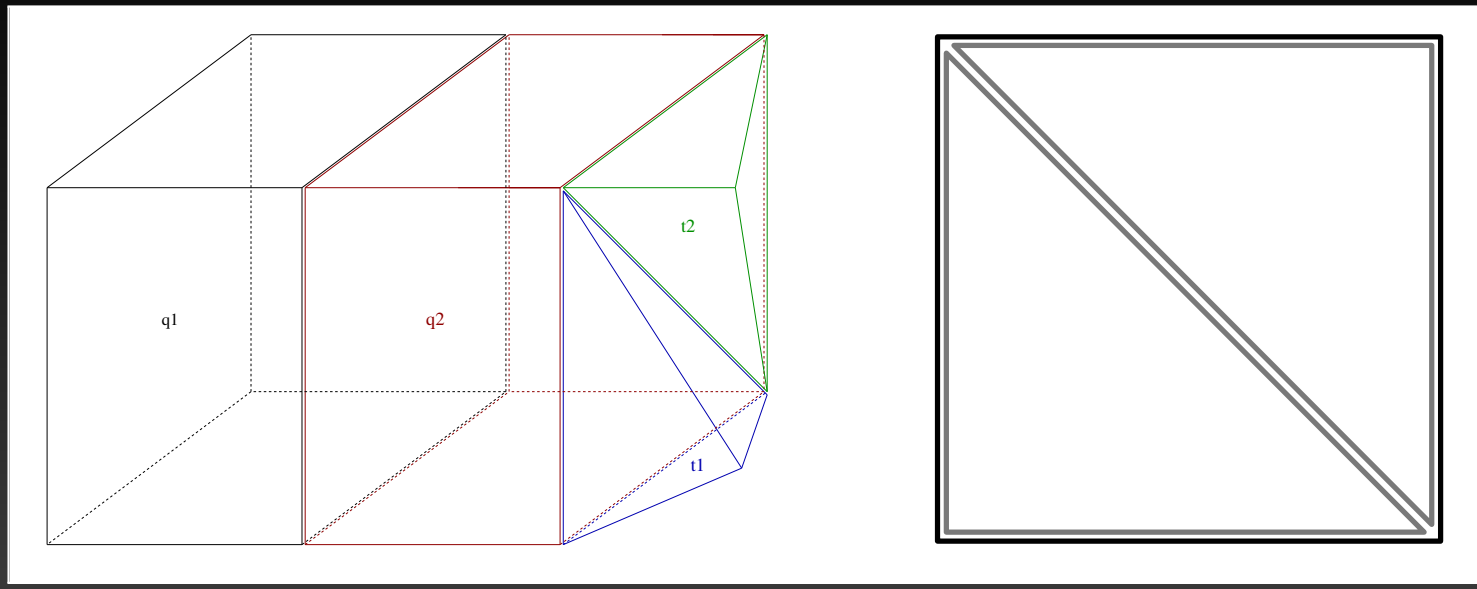

Authorized

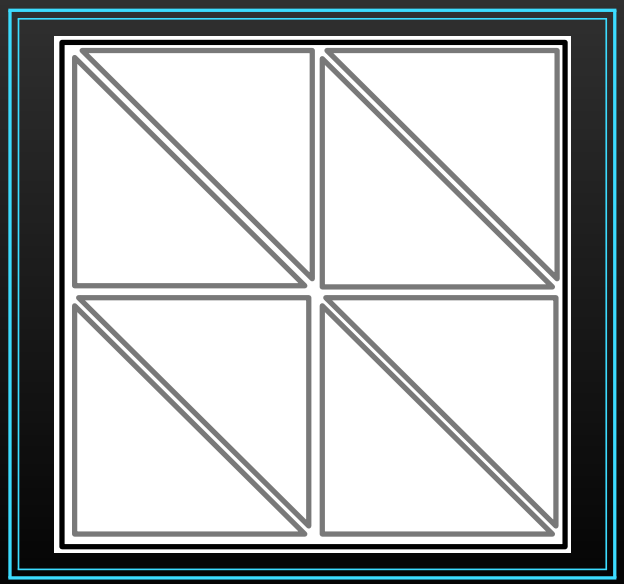

Avoided

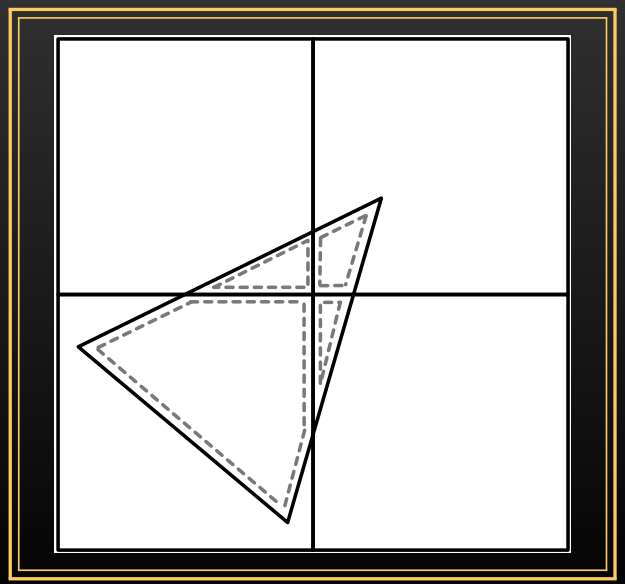

- The discrete solution vector $\mathbf{W}_h$ is searched for in the approximation space V_h^6 defined by :

$$V_h = \left\{ v_h \in L^2(\Omega) \;\middle|\; \begin{array}{l} \forall c_i \in \mathscr{T}_h,\ v_{h|c_i} \in \mathbb{P}_p[c_i] \\ \forall c_i \in \mathscr{Q}_h,\ v_{h|c_i} \in \mathbb{Q}_k[c_i] \end{array} \right\}$$

- $\mathbf{W}_i$ defines the restriction of the approximate solution to the cell c_i ($\mathbf{W}_{h|c_i}$) and local degrees of freedom denoted by $\mathbf{W}_{il} \in \mathbb{R}^6$:

$$\begin{aligned} c_i \in \mathscr{T}_h \quad &\Longrightarrow \quad \mathbf{W}_i \in \mathbb{P}_p[c_i] : \mathbf{W}_i(\mathbf{x}) \quad = \quad \sum_{l=1}^{d_i} \mathbf{W}_{il} \varphi_{il}(\mathbf{x}) \in \mathbb{R}^6 \\ c_i \in \mathscr{Q}_h \quad &\Longrightarrow \quad \mathbf{W}_i \in \mathbb{Q}_k[c_i] : \mathbf{W}_i(\mathbf{x}) \quad = \quad \sum_{l=1}^{b_i} \mathbf{W}_{il} \vartheta_{il}(\mathbf{x}) \in \mathbb{R}^6 \end{aligned}$$

- We use integration by parts on the first weak form and we inject $\mathbf{W}_h$
- The local representation of $\mathbf{W}_h$ does not provide any form of continuity from one element to another. We use a centered numerical flux on $a_{ij} = c_i \cap c_j$:

$$\mathbf{W}_{h|a_{ij}} = \frac{\mathbf{W}_{i|a_{ij}} + \mathbf{W}_{j|a_{ij}}}{2}$$

If a_{ij} on the metallic boundary : $(\mathbf{E}_j, \mathbf{H}_j)^{\mathrm{T}} = (-\mathbf{E}_i, \mathbf{H}_i)^{\mathrm{T}}$

- The discrete solution vector $\mathbf{W}_h$ is searched for in the approximation space V_h^6 defined by :

$$V_h = \left\{ v_h \in L^2(\Omega) \;\middle|\; \begin{array}{l} \forall c_i \in \mathscr{T}_h,\ v_{h|c_i} \in \mathbb{P}_p[c_i] \\ \forall c_i \in \mathscr{Q}_h,\ v_{h|c_i} \in \mathbb{Q}_k[c_i] \end{array} \right\}$$

- $\mathbf{W}_i$ defines the restriction of the approximate solution to the cell c_i ($\mathbf{W}_{h|c_i}$) and local degrees of freedom denoted by $\mathbf{W}_{il} \in \mathbb{R}^6$:

$$\begin{array}{rcl} c_i \in \mathscr{T}_h & \Longrightarrow & \mathbf{W}_i \in \mathbb{P}_p[c_i] : \mathbf{W}_i(\mathbf{x}) = \sum_{l=1}^{d_i} \mathbf{W}_{il}\varphi_{il}(\mathbf{x}) \in \mathbb{R}^6 \\ c_i \in \mathscr{Q}_h & \Longrightarrow & \mathbf{W}_i \in \mathbb{Q}_k[c_i] : \mathbf{W}_i(\mathbf{x}) = \sum_{l=1}^{b_i} \mathbf{W}_{il}\vartheta_{il}(\mathbf{x}) \in \mathbb{R}^6 \end{array}$$

- We use integration by parts on the first weak form and we inject $\mathbf{W}_h$
- The local representation of $\mathbf{W}_h$ does not provide any form of continuity from one element to another. We use a centered numerical flux on $a_{ij} = c_i \cap c_j$:

$$\mathbf{W}_{h|a_{ij}} = \frac{\mathbf{W}_{i|a_{ij}} + \mathbf{W}_{j|a_{ij}}}{2}$$

If a_{ij} on the metallic boundary : $(\mathbf{E}_j, \mathbf{H}_j)^{\mathrm{T}} = (-\mathbf{E}_i, \mathbf{H}_i)^{\mathrm{T}}$

- The discrete solution vector $\mathbf{W}_h$ is searched for in the approximation space V_h^6 defined by :

$$V_h = \left\{ v_h \in L^2(\Omega) \;\middle|\; \begin{array}{l} \forall c_i \in \mathscr{T}_h,\ v_{h|c_i} \in \mathbb{P}_p[c_i] \\ \forall c_i \in \mathscr{Q}_h,\ v_{h|c_i} \in \mathbb{Q}_k[c_i] \end{array} \right\}$$

- $\mathbf{W}_i$ defines the restriction of the approximate solution to the cell c_i ($\mathbf{W}_{h|c_i}$) and local degrees of freedom denoted by $\mathbf{W}_{il} \in \mathbb{R}^6$:

$$\begin{array}{rcl} c_i \in \mathscr{T}_h & \Longrightarrow & \mathbf{W}_i \in \mathbb{P}_p[c_i] : \mathbf{W}_i(\mathbf{x}) = \sum_{l=1}^{d_i} \mathbf{W}_{il}\varphi_{il}(\mathbf{x}) \in \mathbb{R}^6 \\ c_i \in \mathscr{Q}_h & \Longrightarrow & \mathbf{W}_i \in \mathbb{Q}_k[c_i] : \mathbf{W}_i(\mathbf{x}) = \sum_{l=1}^{b_i} \mathbf{W}_{il}\vartheta_{il}(\mathbf{x}) \in \mathbb{R}^6 \end{array}$$

- We use integration by parts on the first weak form and we inject $\mathbf{W}_h$
- The local representation of $\mathbf{W}_h$ does not provide any form of continuity from one element to another. We use a centered numerical flux on $a_{ij} = c_i \cap c_j$:

$$\mathbf{W}_h|_{a_{ij}} = \frac{\mathbf{W}_i|_{a_{ij}} + \mathbf{W}_j|_{a_{ij}}}{2}$$

If a_{ij} on the metallic boundary : $(\mathbf{E}_j, \mathbf{H}_j)^{\mathrm{T}} = (-\mathbf{E}_i, \mathbf{H}_i)^{\mathrm{T}}$

Case (A) :

c_i is a tetrahedron. a_{ij} face of c_i, is **either** on boundary, **or** common to another tetrahedron, **or** to a hexahedron (**hybrid**)

6d$_i$ semi-discretized equations system :

$$\begin{cases} 2\mathcal{X}_{\varepsilon,i}\dfrac{d\overline{\mathbf{E}}_i}{dt} + \displaystyle\sum_{k=1}^{3}\mathcal{X}_i^{x_k}\overline{\mathbf{H}}_i + \sum_{a_{ij}\in\mathscr{T}_d^i}\mathcal{X}_{ij}\overline{\mathbf{H}}_j + \sum_{a_{ij}\in\mathscr{T}_m^i}\mathcal{X}_{im}\overline{\mathbf{H}}_i + \sum_{a_{ij}\in\mathscr{H}_d^i}\mathcal{A}_{ij}\widetilde{\mathbf{H}}_j = 0, \\ 2\mathcal{X}_{\mu,i}\dfrac{d\overline{\mathbf{H}}_i}{dt} - \displaystyle\sum_{k=1}^{3}\mathcal{X}_i^{x_k}\overline{\mathbf{E}}_i - \sum_{a_{ij}\in\mathscr{T}_d^i}\mathcal{X}_{ij}\overline{\mathbf{E}}_j + \sum_{a_{ij}\in\mathscr{T}_m^i}\mathcal{X}_{im}\overline{\mathbf{E}}_i - \sum_{a_{ij}\in\mathscr{H}_d^i}\mathcal{A}_{ij}\widetilde{\mathbf{E}}_j = 0, \end{cases}$$

with :

- $\overline{\mathbf{E}}_i = (\mathbf{E}_{i1}, \mathbf{E}_{i2}, \cdots, \mathbf{E}_{id_i})^{\mathrm{T}}$ and $\overline{\mathbf{H}}_i = (\mathbf{H}_{i1}, \mathbf{H}_{i2}, \cdots, \mathbf{H}_{id_i})^{\mathrm{T}} \in \mathbb{R}^{3d_i}$
- $\widetilde{\mathbf{E}}_j = (\mathbf{E}_{j1}, \mathbf{E}_{j2}, \cdots, \mathbf{E}_{jb_j})^{\mathrm{T}}$ and $\widetilde{\mathbf{H}}_j = (\mathbf{H}_{j1}, \mathbf{H}_{j2}, \cdots, \mathbf{H}_{jb_j})^{\mathrm{T}} \in \mathbb{R}^{3b_j}$
- $\mathcal{X}_{\varepsilon,i}$ and $\mathcal{X}_{\mu,i}$ are mass matrices, $\mathcal{X}_i^{x_k}$ gradient matrix, $\mathcal{X}_{ij}$ surface matrix
  $\Longrightarrow$ All have a $3d_i \times 3d_i$ size, **except** $\mathcal{A}_{ij}$, whose size is $3d_i \times 3b_j$

Case (A) :

c_i is a tetrahedron. a_{ij} face of c_i, is **either** on boundary, **or** common to another tetrahedron, **or** to a hexahedron (**hybrid**)

6d$_i$ semi-discretized equations system :

$$\begin{cases} 2\mathcal{X}_{\varepsilon,i}\dfrac{d\overline{\mathbf{E}}_i}{dt} + \displaystyle\sum_{k=1}^{3}\mathcal{X}_i^{x_k}\overline{\mathbf{H}}_i + \sum_{a_{ij}\in\mathscr{T}_d^i}\mathcal{X}_{ij}\overline{\mathbf{H}}_j + \sum_{a_{ij}\in\mathscr{T}_m^i}\mathcal{X}_{im}\overline{\mathbf{H}}_i + \sum_{a_{ij}\in\mathscr{H}_d^i}\mathcal{A}_{ij}\widetilde{\mathbf{H}}_j = 0, \\ 2\mathcal{X}_{\mu,i}\dfrac{d\overline{\mathbf{H}}_i}{dt} - \displaystyle\sum_{k=1}^{3}\mathcal{X}_i^{x_k}\overline{\mathbf{E}}_i - \sum_{a_{ij}\in\mathscr{T}_d^i}\mathcal{X}_{ij}\overline{\mathbf{E}}_j + \sum_{a_{ij}\in\mathscr{T}_m^i}\mathcal{X}_{im}\overline{\mathbf{E}}_i - \sum_{a_{ij}\in\mathscr{H}_d^i}\mathcal{A}_{ij}\widetilde{\mathbf{E}}_j = 0, \end{cases}$$

with :

- $\overline{\mathbf{E}}_i = (\mathbf{E}_{i1}, \mathbf{E}_{i2}, \cdots, \mathbf{E}_{id_i})^{\mathrm{T}}$ and $\overline{\mathbf{H}}_i = (\mathbf{H}_{i1}, \mathbf{H}_{i2}, \cdots, \mathbf{H}_{id_i})^{\mathrm{T}} \in \mathbb{R}^{3d_i}$
- $\widetilde{\mathbf{E}}_j = (\mathbf{E}_{j1}, \mathbf{E}_{j2}, \cdots, \mathbf{E}_{jb_j})^{\mathrm{T}}$ and $\widetilde{\mathbf{H}}_j = (\mathbf{H}_{j1}, \mathbf{H}_{j2}, \cdots, \mathbf{H}_{jb_j})^{\mathrm{T}} \in \mathbb{R}^{3b_j}$
- $\mathcal{X}_{\varepsilon,i}$ and $\mathcal{X}_{\mu,i}$ are mass matrices, $\mathcal{X}_i^{x_k}$ gradient matrix, $\mathcal{X}_{ij}$ surface matrix $\Longrightarrow$ All have a $3d_i \times 3d_i$ size, **except** $\mathcal{A}_{ij}$, whose size is $3d_i \times 3b_j$

Case (B) :

c_i is an hexahedron. a_{ij} face of c_i, is **either** on boundary, **or** common to another hexahedron, **or** to a tetrahedron (**hybrid**)

$6b_i$ semi-discretized equations system :

$$\begin{cases} 2\mathcal{W}_{\varepsilon,i}\dfrac{d\widetilde{\mathbf{E}}_i}{dt} + \displaystyle\sum_{k=1}^{3}\mathcal{W}_i^{x_k}\widetilde{\mathbf{H}}_i + \sum_{a_{ij}\in\mathscr{Q}_d^i}\mathcal{W}_{ij}\widetilde{\mathbf{H}}_j + \sum_{a_{ij}\in\mathscr{Q}_m^i}\mathcal{W}_{im}\widetilde{\mathbf{H}}_i + \sum_{a_{ij}\in\mathscr{H}_d^i}\mathcal{B}_{ij}\overline{\mathbf{H}}_j = 0, \\ 2\mathcal{W}_{\mu,i}\dfrac{d\widetilde{\mathbf{H}}_i}{dt} - \displaystyle\sum_{k=1}^{3}\mathcal{W}_i^{x_k}\widetilde{\mathbf{E}}_i - \sum_{a_{ij}\in\mathscr{Q}_d^i}\mathcal{W}_{ij}\widetilde{\mathbf{E}}_j + \sum_{a_{ij}\in\mathscr{Q}_m^i}\mathcal{W}_{im}\widetilde{\mathbf{E}}_i - \sum_{a_{ij}\in\mathscr{H}_d^i}\mathcal{B}_{ij}\overline{\mathbf{E}}_j = 0, \end{cases}$$

with :

- $\widetilde{\mathbf{E}}_i = (\mathbf{E}_{i1}, \mathbf{E}_{i2}, \cdots, \mathbf{E}_{ib_i})^{\mathrm{T}}$ and $\widetilde{\mathbf{H}}_i = (\mathbf{H}_{i1}, \mathbf{H}_{i2}, \cdots, \mathbf{H}_{ib_i})^{\mathrm{T}} \in \mathbb{R}^{3b_i}$
- $\overline{\mathbf{E}}_j = (\mathbf{E}_{j1}, \mathbf{E}_{j2}, \cdots, \mathbf{E}_{jd_j})^{\mathrm{T}}$ and $\overline{\mathbf{H}}_j = (\mathbf{H}_{j1}, \mathbf{H}_{j2}, \cdots, \mathbf{H}_{jd_j})^{\mathrm{T}} \in \mathbb{R}^{3d_j}$
- $\mathcal{W}_{\varepsilon,i}$ and $\mathcal{W}_{\mu,i}$ are mass matrices, $\mathcal{W}_i^{x_k}$ gradient matrix, $\mathcal{W}_{ij}$ surface matrix $\Longrightarrow$ All have a $3b_i \times 3b_i$ size, **except** $\mathcal{B}_{ij}$, whose size is $3b_i \times 3d_j$

Second order Leap-Frog scheme

$$\begin{cases} \overline{\mathbf{H}}_i^{n+\frac{1}{2}} = \overline{\mathbf{H}}_i^{n-\frac{1}{2}} + \Delta t\, \overline{v}_{\tau_i}\Big(G_{el}\big(\mathbf{E}_h^n\big)\Big), \\ \overline{\mathbf{E}}_i^{n+1} = \overline{\mathbf{E}}_i^{n} + \Delta t\, \overline{v}_{\tau_i}\Big(G_{mag}\Big(\mathbf{H}_h^{n+\frac{1}{2}}\Big)\Big) \end{cases}$$

Fourth order Leap-Frog scheme [15]

$$\begin{cases} \overline{\mathbf{H}}_i^{n+\frac{1}{2}} = \overline{\mathbf{H}}_i^{n-\frac{1}{2}} + \Delta t\, \overline{v}_{\tau_i}\Big(G_{el}\big(\mathbf{E}_h^n\big)\Big) + \dfrac{\Delta t^3}{24}\ \overline{v}_{\tau_i}\Big(G_{el}\circ G_{mag}\circ G_{el}\big(\mathbf{E}_h^n\big)\Big), \\ \overline{\mathbf{E}}_i^{n+1} = \overline{\mathbf{E}}_i^{n} + \Delta t\, \overline{v}_{\tau_i}\Big(G_{mag}\Big(\mathbf{H}_h^{n+\frac{1}{2}}\Big)\Big) + \dfrac{\Delta t^3}{24}\ \overline{v}_{\tau_i}\Big(G_{mag}\circ G_{el}\circ G_{mag}\Big(\mathbf{H}_h^{n+\frac{1}{2}}\Big)\Big) \end{cases}$$

[15] H. Fahs.
High-order Leap-Frog based discontinuous Galerkin method for the time-domain Maxwell equations on non-conforming simplicial meshes.
Numer. Math. Theor. Meth. Appl., vol. 2, no. 3, pp. 275–300, 2009.

Second order Leap-Frog scheme

$$\begin{cases} \overline{\mathbf{H}}_i^{n+\frac{1}{2}} = \overline{\mathbf{H}}_i^{n-\frac{1}{2}} + \Delta t\, \overline{\upsilon}_{\tau_i}\Big(G_{el}\big(\mathbf{E}_h^n\big)\Big), \\ \overline{\mathbf{E}}_i^{n+1} = \overline{\mathbf{E}}_i^{n} + \Delta t\, \overline{\upsilon}_{\tau_i}\Big(G_{mag}\Big(\mathbf{H}_h^{n+\frac{1}{2}}\Big)\Big) \end{cases}$$

Fourth order Leap-Frog scheme [15]

$$\begin{cases} \overline{\mathbf{H}}_i^{n+\frac{1}{2}} = \overline{\mathbf{H}}_i^{n-\frac{1}{2}} + \Delta t\, \overline{\upsilon}_{\tau_i}\Big(G_{el}\big(\mathbf{E}_h^n\big)\Big) + \dfrac{\Delta t^3}{24}\ \overline{\upsilon}_{\tau_i}\Big(G_{el}\circ G_{mag}\circ G_{el}\big(\mathbf{E}_h^n\big)\Big), \\ \overline{\mathbf{E}}_i^{n+1} = \overline{\mathbf{E}}_i^{n} + \Delta t\, \overline{\upsilon}_{\tau_i}\Big(G_{mag}\Big(\mathbf{H}_h^{n+\frac{1}{2}}\Big)\Big) + \dfrac{\Delta t^3}{24}\ \overline{\upsilon}_{\tau_i}\Big(G_{mag}\circ G_{el}\circ G_{mag}\Big(\mathbf{H}_h^{n+\frac{1}{2}}\Big)\Big) \end{cases}$$

[15] H. Fahs.
High-order Leap-Frog based discontinuous Galerkin method for the time-domain Maxwell equations on non-conforming simplicial meshes.
Numer. Math. Theor. Meth. Appl., vol. 2, no. 3, pp. 275–300, 2009.

Outline

- We define a discrete energy $\mathfrak{E}^n$
- We assume that this is an energy and we check that it is exactly conserved, i.e. $\Delta\mathfrak{E} = \mathfrak{E}^{n+1} - \mathfrak{E}^n = 0$
- We make hypotheses for fields to prove that $\mathfrak{E}^n$ is a positive definite quadratic form under a CFL condition :

$$\forall \mathbf{X} \in \left(\mathbb{P}_p[c_i]\right)^3, \quad \|\mathrm{curl}(\mathbf{X})\|_{c_i} \leq \left(\alpha_i^\tau p_i \|\mathbf{X}\|_{c_i}\right)/|c_i|,$$

$$\forall \mathbf{X} \in \left(\mathbb{P}_p[c_i]\right)^3, \quad \|\mathbf{X}\|_{a_{ij}}^2 \leq \left(\beta_{ij}^\tau \|\mathbf{n}_{ij}\| \|\mathbf{X}\|_{c_i}^2\right)/|c_i|$$

  where α_i^τ and β_{ij}^τ $(j \in \{j | c_i \cap c_j \neq \varnothing\})$ defining the constant parameters

- We also admit similar hypothesis $\forall \mathbf{X} \in \left(\mathbb{Q}_k[c_i]\right)^3$ with constants α_i^q and β_{ij}^q
- $\|.\|_{c_i}$ and $\|.\|_{a_{ij}}$ are L^2-norm. $\|\mathbf{n}_{ij}\| = \int_{a_{ij}} 1 d\sigma$ with $\mathbf{n}_{ij}$ non-unitary normal to a_{ij} oriented from c_i towards c_j. $|c_i| = \int_{c_i} 1 d\mathbf{x}$ and $p_i = \sum_{j \in \mathcal{V}_i} \|\mathbf{n}_{ij}\|$

- We define a discrete energy $\mathfrak{E}^n$
- We assume that this is an energy and we check that it is exactly conserved, i.e. $\Delta\mathfrak{E} = \mathfrak{E}^{n+1} - \mathfrak{E}^n = 0$
- We make hypotheses for fields to prove that $\mathfrak{E}^n$ is a positive definite quadratic form under a CFL condition :

$$\forall \mathbf{X} \in (\mathbb{P}_p[c_i])^3, \quad \|\mathrm{curl}(\mathbf{X})\|_{c_i} \leq (\alpha_i^\tau p_i \|\mathbf{X}\|_{c_i}) / |c_i|,$$

$$\forall \mathbf{X} \in (\mathbb{P}_p[c_i])^3, \quad \|\mathbf{X}\|_{a_{ij}}^2 \leq (\beta_{ij}^\tau \|\mathbf{n}_{ij}\| \|\mathbf{X}\|_{c_i}^2) / |c_i|$$

  where α_i^τ and β_{ij}^τ $(j \in \{j | c_i \cap c_j \neq \varnothing\})$ defining the constant parameters

- We also admit similar hypothesis $\forall \mathbf{X} \in (\mathbb{Q}_k[c_i])^3$ with constants α_i^q and β_{ij}^q
- $\|.\|_{c_i}$ and $\|.\|_{a_{ij}}$ are L^2-norm. $\|\mathbf{n}_{ij}\| = \int_{a_{ij}} 1 d\sigma$ with $\mathbf{n}_{ij}$ non-unitary normal to a_{ij} oriented from c_i towards c_j. $|c_i| = \int_{c_i} 1 d\mathbf{x}$ and $p_i = \sum_{j \in \mathcal{V}_i} \|\mathbf{n}_{ij}\|$

- For the DGTD-$\mathbb{P}_p$ method, the sufficient condition on Δt_τ is [16] :

$$\forall i, \forall j \in \mathcal{V}_i : \quad \Delta t_\tau \left[2\alpha_i^\tau + \beta_{ij}^\tau \max\left(\sqrt{\frac{\varepsilon_i}{\varepsilon_j}}, \sqrt{\frac{\mu_i}{\mu_j}} \right) \right] < \frac{4|c_i|\sqrt{\varepsilon_i \mu_i}}{p_i}$$

- For DGTD-$\mathbb{Q}_k$ method, the sufficient condition on Δt_q is :

$$\forall i, \forall j \in \mathcal{V}_i : \quad \Delta t_q \left[2\alpha_i^q + \beta_{ij}^q \max\left(\sqrt{\frac{\varepsilon_i}{\varepsilon_j}}, \sqrt{\frac{\mu_i}{\mu_j}} \right) \right] < \frac{4|c_i|\sqrt{\varepsilon_i \mu_i}}{p_i}$$

Finally, denoting Δt the global time step for the hybrid method, we have shown that the sufficient stability condition is defined by :

$$\Delta t = \min(\Delta t_\tau, \Delta t_q)$$

Under this condition and hypothesis, $\mathfrak{E}^n$ is a positive definite quadratic form

[16] L. Fezoui, S. Lanteri, S. Lohrengel, and S. Piperno.
Convergence and stability of a discontinuous Galerkin time-domain method for the heterogeneous Maxwell equations on unstructured meshes.
ESAIM : Math. Model. and Numer. Anal. 39, no. 6, pp. 1149–1176, 2005.

- For the DGTD-$\mathbb{P}_p$ method, the sufficient condition on Δt_τ is [16] :

$$\forall i, \forall j \in \mathcal{V}_i : \quad \Delta t_\tau \left[2\alpha_i^\tau + \beta_{ij}^\tau \max\left(\sqrt{\frac{\varepsilon_i}{\varepsilon_j}}, \sqrt{\frac{\mu_i}{\mu_j}} \right) \right] < \frac{4|c_i|\sqrt{\varepsilon_i \mu_i}}{p_i}$$

- For DGTD-$\mathbb{Q}_k$ method, the sufficient condition on Δt_q is :

$$\forall i, \forall j \in \mathcal{V}_i : \quad \Delta t_q \left[2\alpha_i^q + \beta_{ij}^q \max\left(\sqrt{\frac{\varepsilon_i}{\varepsilon_j}}, \sqrt{\frac{\mu_i}{\mu_j}} \right) \right] < \frac{4|c_i|\sqrt{\varepsilon_i \mu_i}}{p_i}$$

Finally, denoting Δt the global time step for the hybrid method, we have shown that the sufficient stability condition is defined by :

$$\boxed{\Delta t = \min(\Delta t_\tau, \Delta t_q)}$$

Under this condition and hypothesis, $\mathfrak{E}^n$ is a positive definite quadratic form

---

[16] L. Fezoui, S. Lanteri, S. Lohrengel, and S. Piperno.
Convergence and stability of a discontinuous Galerkin time-domain method for the heterogeneous Maxwell equations on unstructured meshes.
ESAIM : Math. Model. and Numer. Anal. 39, no. 6, pp. 1149–1176, 2005.

- Scalar weak formulations per element for the two cases
- Summing up weak formulations on each c_i, the discrete solution $\mathbf{W}_h = (\mathbf{E}_h, \mathbf{H}_h)^{\mathrm{T}} \in \mathcal{C}^1([0, t_f]; V_h^6)$ satisfies :

$$m(\partial_t \mathbf{W}_h, \mathbf{T}') + a(\mathbf{W}_h, \mathbf{T}') + b(\mathbf{W}_h, \mathbf{T}') = 0, \quad \forall \mathbf{T}' \in V_h^6$$

where :

$$\begin{cases} m(\mathbf{T}, \mathbf{T}') = 2 \displaystyle\int_\Omega \langle Q\mathbf{T} \, , \, \mathbf{T}' \rangle d\mathbf{x} \\ a(\mathbf{T}, \mathbf{T}') = \displaystyle\int_\Omega \left(\left\langle \sum_{k=1}^{3} \partial_{x_k}^h \mathcal{O}^k \mathbf{T} \, , \, \mathbf{T}' \right\rangle - \sum_{k=1}^{3} \langle \partial_{x_k}^h \mathbf{T}' \, , \, \mathcal{O}^k \mathbf{T} \rangle \right) d\mathbf{x} \\ b(\mathbf{T}, \mathbf{T}') = \displaystyle\int_{\mathscr{F}_d} \big(\langle \{\mathbf{V}\} \, , \, [\![\mathbf{U}']\!] \rangle - \langle \{\mathbf{U}\} \, , \, [\![\mathbf{V}']\!] \rangle - \\ \qquad \langle \{\mathbf{V}'\} \, , \, [\![\mathbf{U}]\!] \rangle + \langle \{\mathbf{U}'\} \, , \, [\![\mathbf{V}]\!] \rangle \big) \, d\sigma + \\ \qquad \displaystyle\int_{\mathscr{F}_m} \big(\langle \mathbf{U} \, , \, \check{\mathbf{n}} \times \mathbf{V}' \rangle + \langle \mathbf{V} \, , \, \check{\mathbf{n}} \times \mathbf{U}' \rangle \big) \, d\sigma \end{cases}$$

with :

- $\mathbf{T} = (\mathbf{U}, \mathbf{V})^{\mathrm{T}}$, $\mathbf{T}' = (\mathbf{U}', \mathbf{V}')^{\mathrm{T}}$
- $[\![\mathbf{U}_h]\!]_{ij} = \left(\mathbf{U}_j|_{a_{ij}} - \mathbf{U}_i|_{a_{ij}} \right) \times \check{\mathbf{n}}_{ij}$, $\{\mathbf{U}_h\}_{ij} = \left(\mathbf{U}_i|_{a_{ij}} + \mathbf{U}_j|_{a_{ij}} \right)/2$
- $\mathscr{F}_d$ set of internal faces, $\mathscr{F}_m$ set of metallic boundary faces

- Scalar weak formulations per element for the two cases
- Summing up weak formulations on each c_i, the discrete solution $\mathbf{W}_h = (\mathbf{E}_h, \mathbf{H}_h)^{\mathrm{T}} \in \mathcal{C}^1([0, t_f]; V_h^6)$ satisfies :

$$m(\partial_t \mathbf{W}_h, \mathbf{T}') + a(\mathbf{W}_h, \mathbf{T}') + b(\mathbf{W}_h, \mathbf{T}') = 0, \quad \forall \mathbf{T}' \in V_h^6$$

where :

$$\begin{cases} m(\mathbf{T}, \mathbf{T}') = 2 \displaystyle\int_\Omega \langle Q\mathbf{T} \ , \ \mathbf{T}' \rangle d\mathbf{x} \\ a(\mathbf{T}, \mathbf{T}') = \displaystyle\int_\Omega \left(\left\langle \sum_{k=1}^{3} \partial_{x_k}^h \mathcal{O}^k \mathbf{T} \ , \ \mathbf{T}' \right\rangle - \sum_{k=1}^{3} \langle \partial_{x_k}^h \mathbf{T}' \ , \ \mathcal{O}^k \mathbf{T} \rangle \right) d\mathbf{x} \\ b(\mathbf{T}, \mathbf{T}') = \displaystyle\int_{\mathscr{F}_d} \left(\langle \{\mathbf{V}\} \ , \ [\![\mathbf{U}']\!] \rangle - \langle \{\mathbf{U}\} \ , \ [\![\mathbf{V}']\!] \rangle - \right. \\ \qquad \left. \langle \{\mathbf{V}'\} \ , \ [\![\mathbf{U}]\!] \rangle + \langle \{\mathbf{U}'\} \ , \ [\![\mathbf{V}]\!] \rangle \right) d\sigma + \\ \qquad \displaystyle\int_{\mathscr{F}_m} \left(\langle \mathbf{U} \ , \ \check{\mathbf{n}} \times \mathbf{V}' \rangle + \langle \mathbf{V} \ , \ \check{\mathbf{n}} \times \mathbf{U}' \rangle \right) d\sigma \end{cases}$$

with :

- $\mathbf{T} = (\mathbf{U}, \mathbf{V})^{\mathrm{T}}$, $\mathbf{T}' = (\mathbf{U}', \mathbf{V}')^{\mathrm{T}}$
- $[\![\mathbf{U}_h]\!]_{ij} = \left(\mathbf{U}_j|_{a_{ij}} - \mathbf{U}_i|_{a_{ij}} \right) \times \check{\mathbf{n}}_{ij}$, $\{\mathbf{U}_h\}_{ij} = \left(\mathbf{U}_i|_{a_{ij}} + \mathbf{U}_j|_{a_{ij}} \right)/2$
- $\mathscr{F}_d$ set of internal faces, $\mathscr{F}_m$ set of metallic boundary faces

- Let the exact solution $\mathbf{W} \in \mathcal{C}^1([0,t_f],(L^2(\Omega))^6) \bigcap \mathcal{C}^0([0,t_f],(H(\mathrm{curl},\Omega))^6)$. Using the continuity of the tangential traces of $\mathbf{E}$ and $\mathbf{H}$ across $a_{ij} \in \mathscr{F}_d$, and the metallic boundary condition $\mathbf{E} \times \check{\mathbf{n}} = 0$ on $a_{ij} \in \mathscr{F}_m$, we prove :

$$m(\partial_t \mathbf{W}, \mathbf{T}') + a(\mathbf{W}, \mathbf{T}') + b(\mathbf{W}, \mathbf{T}') = 0, \quad \forall \mathbf{T}' \in V_h^6$$

- We also make several assumptions and that $\mathbf{W} \in \mathcal{C}^0([0,t_f];(PH^{s+1}(\Omega))^6)$ for $s \leq 0$ with t_f the final time and :

$$PH^{s+1}(\Omega) = \{v \mid \forall j, v_{|\Omega_j} \in H^{s+1}(\Omega_j)\}$$

- Let $h_\tau = \max\limits_{\tau_i \in \mathscr{T}_h}(h_{\tau_i})$, $h_q = \max\limits_{q_i \in \mathscr{Q}_h}(h_{q_i})$ and :

$$\xi_h = \max\left\{h_\tau^{\min\{s,p\}}, h_q^{\min\{s,k\}}\right\}$$

- Then there is a constant $C > 0$ independent of h such that :

$$\max_{t\in[0,t_f]}\left(\|P_h(\mathbf{W}(t)) - \mathbf{W}_h(t)\|_{0,\Omega}\right) \leq C\ \xi_h\ t_f\ \|\mathbf{W}\|_{\mathcal{C}^0([0,t_f],PH^{s+1}(\Omega))}$$

- Let the exact solution $\mathbf{W} \in \mathcal{C}^1([0,t_f],(L^2(\Omega))^6) \bigcap \mathcal{C}^0([0,t_f],(H(\mathrm{curl},\Omega))^6)$. Using the continuity of the tangential traces of $\mathbf{E}$ and $\mathbf{H}$ across $a_{ij} \in \mathscr{F}_d$, and the metallic boundary condition $\mathbf{E} \times \check{\mathbf{n}} = 0$ on $a_{ij} \in \mathscr{F}_m$, we prove :

$$m(\partial_t \mathbf{W}, \mathbf{T}') + a(\mathbf{W}, \mathbf{T}') + b(\mathbf{W}, \mathbf{T}') = 0, \quad \forall \mathbf{T}' \in V_h^6$$

- We also make several assumptions and that $\mathbf{W} \in \mathcal{C}^0([0,t_f];(PH^{s+1}(\Omega))^6)$ for $s \leq 0$ with t_f the final time and :

$$PH^{s+1}(\Omega) = \{v \mid \forall j, v_{|\Omega_j} \in H^{s+1}(\Omega_j)\}$$

- Let $h_\tau = \max\limits_{\tau_i \in \mathscr{T}_h}(h_{\tau_i})$, $h_q = \max\limits_{q_i \in \mathscr{Q}_h}(h_{q_i})$ and :

$$\xi_h = \max\left\{h_\tau^{\min\{s,p\}}, h_q^{\min\{s,k\}}\right\}$$

- Then there is a constant $C > 0$ independent of h such that :

$$\max_{t\in[0,t_f]}\left(\|P_h(\mathbf{W}(t)) - \mathbf{W}_h(t)\|_{0,\Omega}\right) \leq C\ \xi_h\ t_f\ \|\mathbf{W}\|_{\mathcal{C}^0([0,t_f],PH^{s+1}(\Omega))}$$

- Let the exact solution $\mathbf{W} \in \mathcal{C}^1([0,t_f],(L^2(\Omega))^6) \bigcap \mathcal{C}^0([0,t_f],(H(\mathrm{curl},\Omega))^6)$. Using the continuity of the tangential traces of $\mathbf{E}$ and $\mathbf{H}$ across $a_{ij} \in \mathscr{F}_d$, and the metallic boundary condition $\mathbf{E} \times \check{\mathbf{n}} = 0$ on $a_{ij} \in \mathscr{F}_m$, we prove :

$$m(\partial_t \mathbf{W}, \mathbf{T}') + a(\mathbf{W}, \mathbf{T}') + b(\mathbf{W}, \mathbf{T}') = 0, \quad \forall \mathbf{T}' \in V_h^6$$

- We also make several assumptions and that $\mathbf{W} \in \mathcal{C}^0([0,t_f];(PH^{s+1}(\Omega))^6)$ for $s \leq 0$ with t_f the final time and :

$$PH^{s+1}(\Omega) = \{v \mid \forall j, v_{|\Omega_j} \in H^{s+1}(\Omega_j)\}$$

- Let $h_\tau = \max\limits_{\tau_i \in \mathscr{T}_h}(h_{\tau_i})$, $h_q = \max\limits_{q_i \in \mathscr{Q}_h}(h_{q_i})$ and :

$$\xi_h = \max\left\{ h_\tau^{\min\{s,p\}}, h_q^{\min\{s,k\}} \right\}$$

- Then there is a constant $C > 0$ independent of h such that :

$$\max_{t\in[0,t_f]} \left(\|P_h(\mathbf{W}(t)) - \mathbf{W}_h(t)\|_{0,\Omega} \right) \leq C\, \xi_h\, t_f\, \|\mathbf{W}\|_{\mathcal{C}^0([0,t_f],PH^{s+1}(\Omega))}$$

- For the semi-discretized problem, the error $\mathbf{w} = \mathbf{W} - \mathbf{W}_h$ satisfies the estimate :

$$\|\mathbf{w}\|_{\mathcal{C}^0([0,t_f],L^2(\Omega))} \leq C\ \xi_h\ t_f\ \|\mathbf{W}\|_{\mathcal{C}^0([0,t_f],PH^{s+1}(\Omega))}$$

- The fully discretized scheme may be seen as the discretization in time of a system of ODE. Since the Leap-Frog scheme is second-order (fourth-order, respectively) accurate, we found the consistency error altogether of order $\mathcal{O}(\Delta t^2)$ (of order $\mathcal{O}(\Delta t^4)$, respectively).
- Finally, together with the stability result we thus get an error of order (if the exact solution is regular enough) for the LF2 scheme :

$$\mathcal{O}(\Delta t^2) + \mathcal{O}(\xi_h)$$

- And for the LF4 scheme :

$$\mathcal{O}(\Delta t^4) + \mathcal{O}(\xi_h)$$

- For the semi-discretized problem, the error $\mathbf{w} = \mathbf{W} - \mathbf{W}_h$ satisfies the estimate :

$$\|\mathbf{w}\|_{\mathcal{C}^0([0,t_f],L^2(\Omega))} \leq C\ \xi_h\ t_f\ \|\mathbf{W}\|_{\mathcal{C}^0([0,t_f],PH^{s+1}(\Omega))}$$

- The fully discretized scheme may be seen as the discretization in time of a system of ODE. Since the Leap-Frog scheme is second-order (fourth-order, respectively) accurate, we found the consistency error altogether of order $\mathcal{O}(\Delta t^2)$ (of order $\mathcal{O}(\Delta t^4)$, respectively).
- Finally, together with the stability result we thus get an error of order (if the exact solution is regular enough) for the LF2 scheme :

$$\mathcal{O}(\Delta t^2) + \mathcal{O}(\xi_h)$$

- And for the LF4 scheme :

$$\mathcal{O}(\Delta t^4) + \mathcal{O}(\xi_h)$$

- For the semi-discretized problem, the error $\mathbf{w} = \mathbf{W} - \mathbf{W}_h$ satisfies the estimate :

$$\|\mathbf{w}\|_{\mathcal{C}^0([0,t_f],L^2(\Omega))} \leq C\ \xi_h\ t_f\ \|\mathbf{W}\|_{\mathcal{C}^0([0,t_f],PH^{s+1}(\Omega))}$$

- The fully discretized scheme may be seen as the discretization in time of a system of ODE. Since the Leap-Frog scheme is second-order (fourth-order, respectively) accurate, we found the consistency error altogether of order $\mathcal{O}(\Delta t^2)$ (of order $\mathcal{O}(\Delta t^4)$, respectively).

- Finally, together with the stability result we thus get an error of order (if the exact solution is regular enough) for the LF2 scheme :

$$\mathcal{O}(\Delta t^2) + \mathcal{O}(\xi_h)$$

- And for the LF4 scheme :

$$\mathcal{O}(\Delta t^4) + \mathcal{O}(\xi_h)$$

Outline

- 2D transverse magnetic waves (TM_z) : $\mathbf{H} \equiv (H_x, H_y, 0)^{\mathrm{T}}$ et $\mathbf{E} \equiv (0, 0, E_z)^{\mathrm{T}}$
- 2D Maxwell's equations are given by :

$$\begin{cases} \varepsilon \partial_t E_z - \partial_{x_1} H_y + \partial_{x_2} H_x &= 0, \\ \mu \partial_t H_x + \partial_{x_2} E_z &= 0, \\ \mu \partial_t H_y - \partial_{x_1} E_z &= 0. \end{cases}$$

- Classical Lagrange nodal basis functions
- Numerical Gauss-Legendre cubature formulas only for integrals in non-conforming matrices
- Each time step used in the DGTD-$\mathbb{P}_p\mathbb{Q}_k$ (for all the test problems) is the minimum between the limit time step for DGTD-$\mathbb{P}_p$ and the one for DGTD-$\mathbb{Q}_k$ $\Longrightarrow$ numerical validation of the stability analysis

- 2D transverse magnetic waves (TM_z) : $\mathbf{H} \equiv (H_x, H_y, 0)^{\mathrm{T}}$ et $\mathbf{E} \equiv (0, 0, E_z)^{\mathrm{T}}$
- 2D Maxwell's equations are given by :

$$\begin{cases} \varepsilon \partial_t E_z - \partial_{x_1} H_y + \partial_{x_2} H_x &= 0, \\ \mu \partial_t H_x + \partial_{x_2} E_z &= 0, \\ \mu \partial_t H_y - \partial_{x_1} E_z &= 0. \end{cases}$$

- Classical Lagrange nodal basis functions
- Numerical Gauss-Legendre cubature formulas only for integrals in non-conforming matrices
- Each time step used in the DGTD-$\mathbb{P}_p\mathbb{Q}_k$ (for all the test problems) is the minimum between the limit time step for DGTD-$\mathbb{P}_p$ and the one for DGTD-$\mathbb{Q}_k$ $\Longrightarrow$ numerical validation of the stability analysis

- We compute the evolution of the (1,1) mode in a PEC square cavity
- $\Omega = [0,1] \times [0,1]$
- Metallic boundary condition
- The exact solution is :

$$\begin{cases} H_x(x_1, x_2, t) &= -\dfrac{\pi}{\omega} \sin(\pi x_1) \cos(\pi x_2) \sin(\omega t), \\ H_y(x_1, x_2, t) &= \dfrac{\pi}{\omega} \cos(\pi x_1) \sin(\pi x_2) \sin(\omega t), \\ E_z(x_1, x_2, t) &= \sin(\pi x_1) \sin(\pi x_2) \cos(\omega t), \end{cases}$$

where $\omega = 2\pi f$, with f the frequency equal to $f = 212$ MHz

Eigenmode in a unitary PEC square cavity

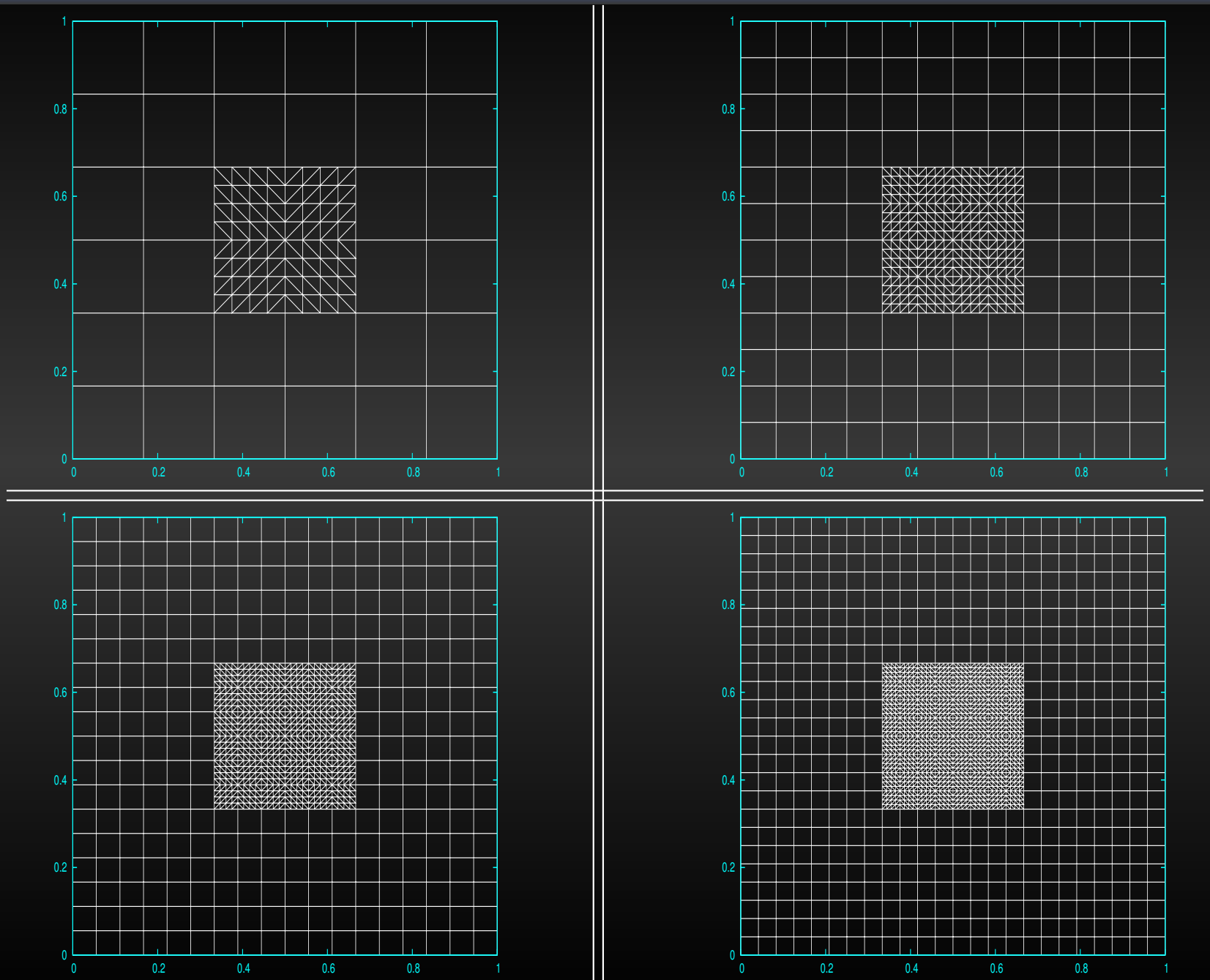

Numerical h-wise convergence for the second-order Leap-Frog scheme :

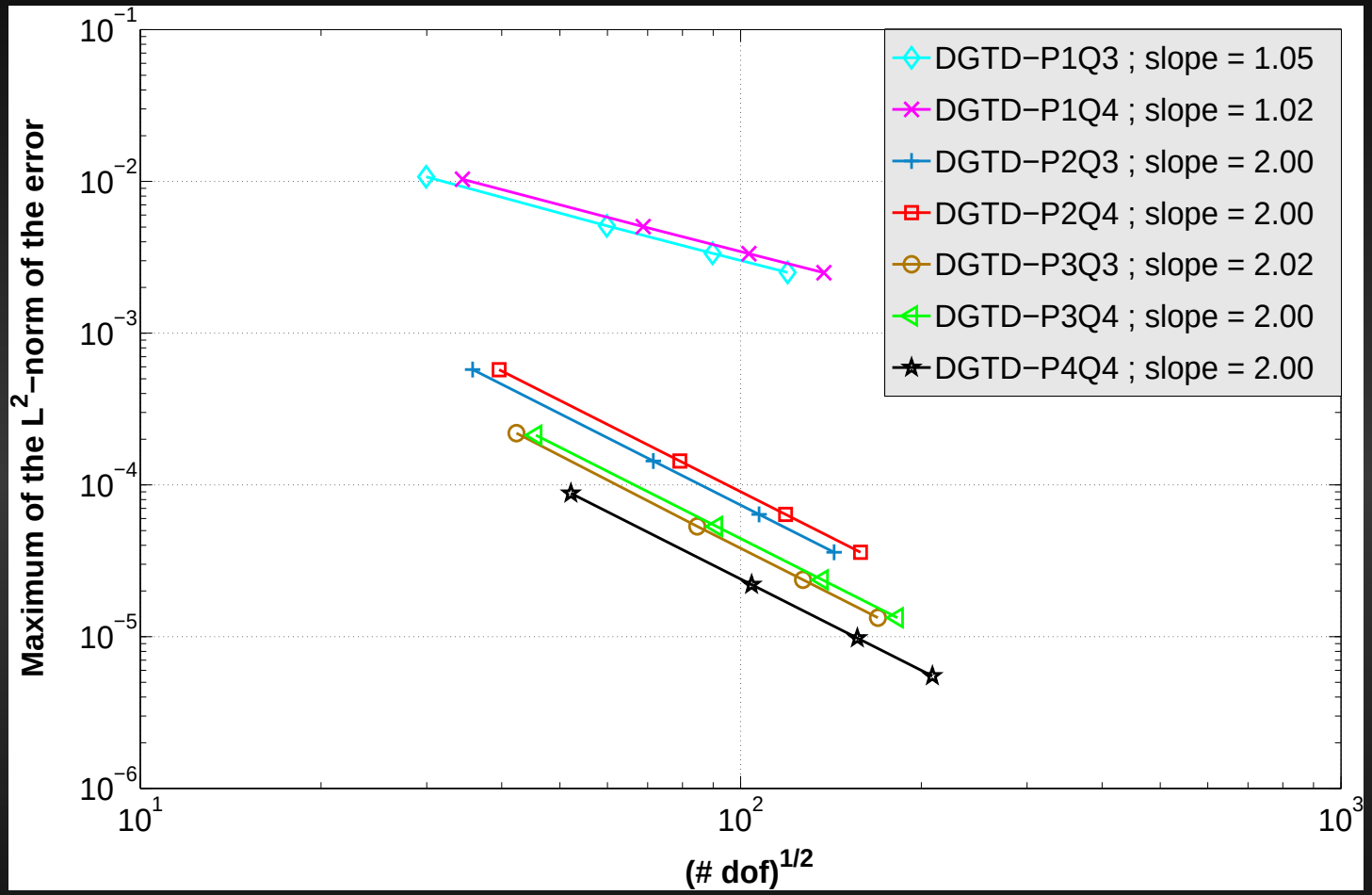

- Numerical validation of convergence in h. Stable method.
- Convergence order limited by LF2.

Numerical h-wise convergence for the fourth-order Leap-Frog scheme :

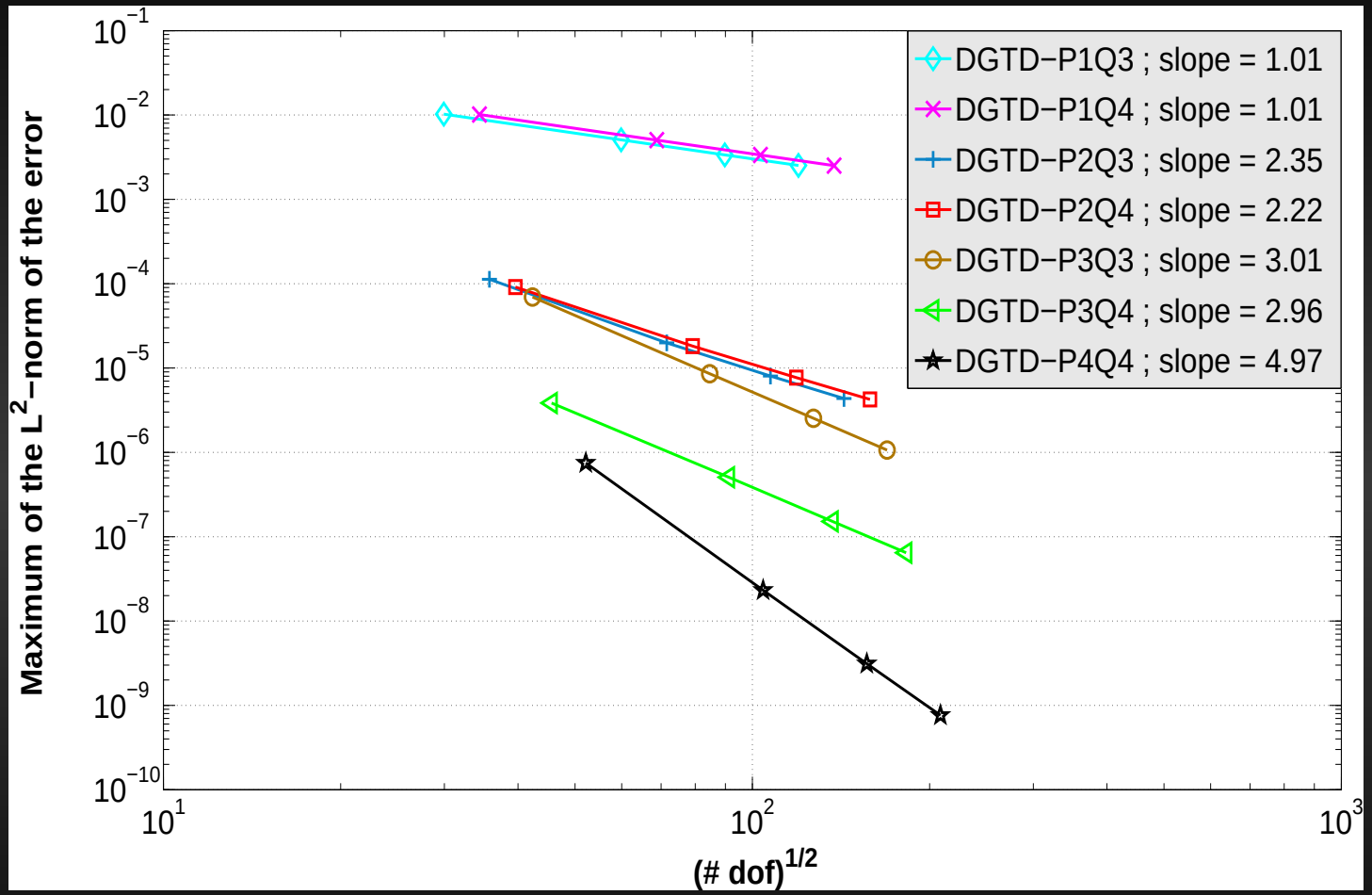

- Numerical validation of convergence in h. Stable method.
- LF4 more efficient and more accurate than LF2 for this test problem.

L^2-error, as a function of CPU time. LF2 (top) and LF4 (bottom) schemes :

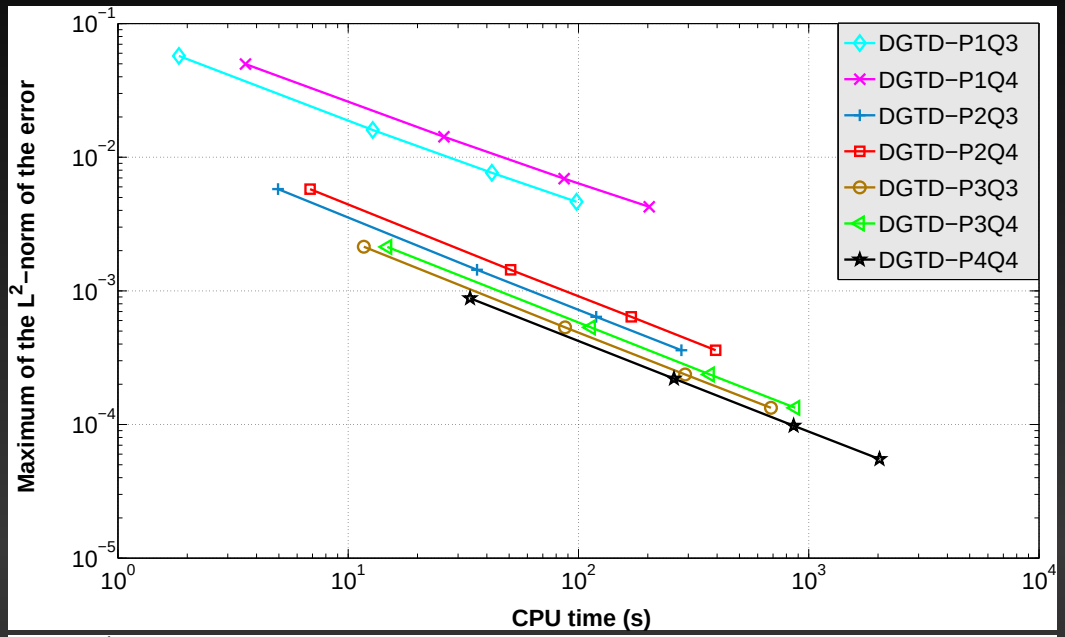

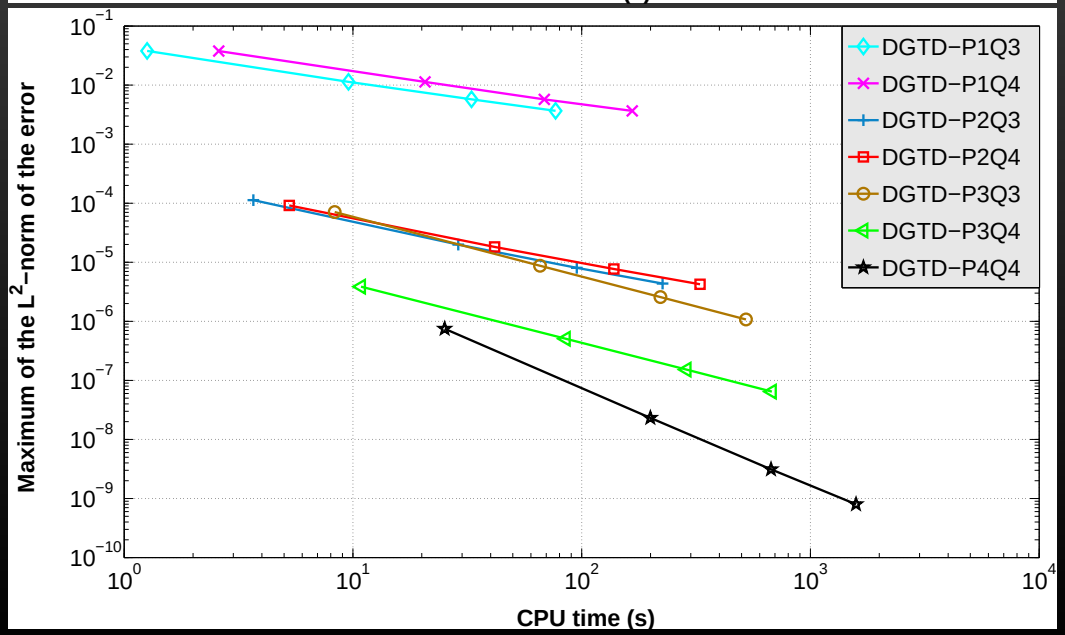

Eigenmode in a unitary PEC square cavity

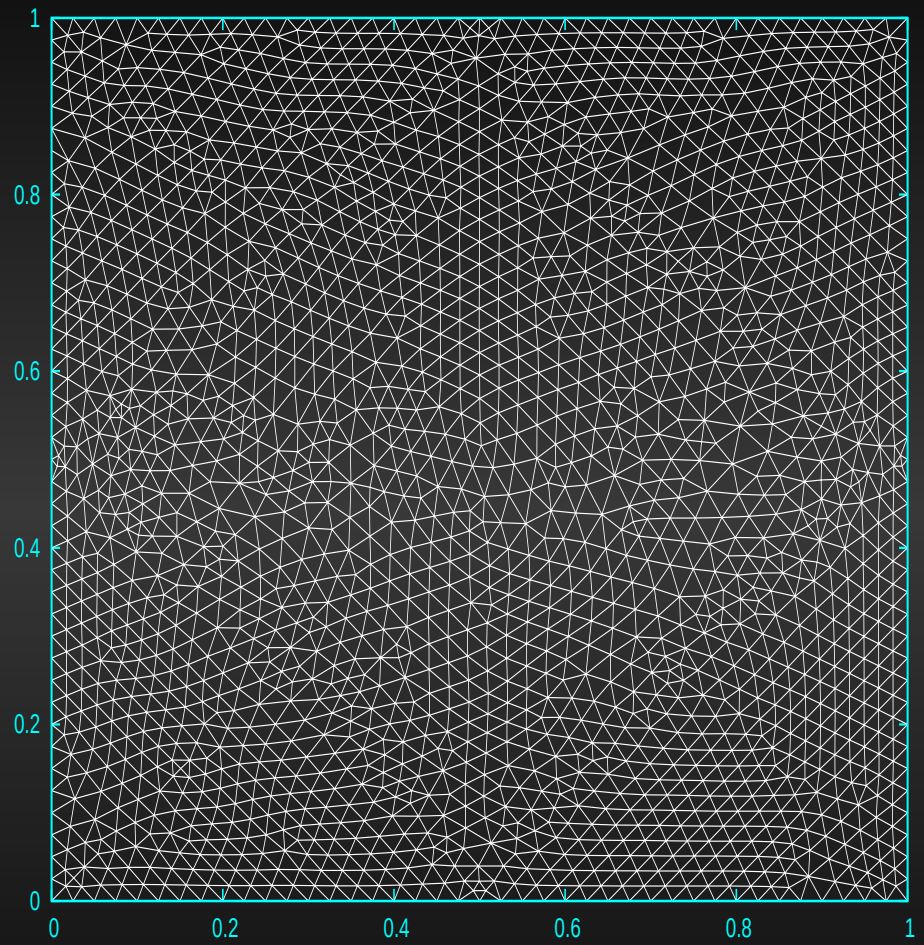

Triangles : 3778
Quadrangles : 0

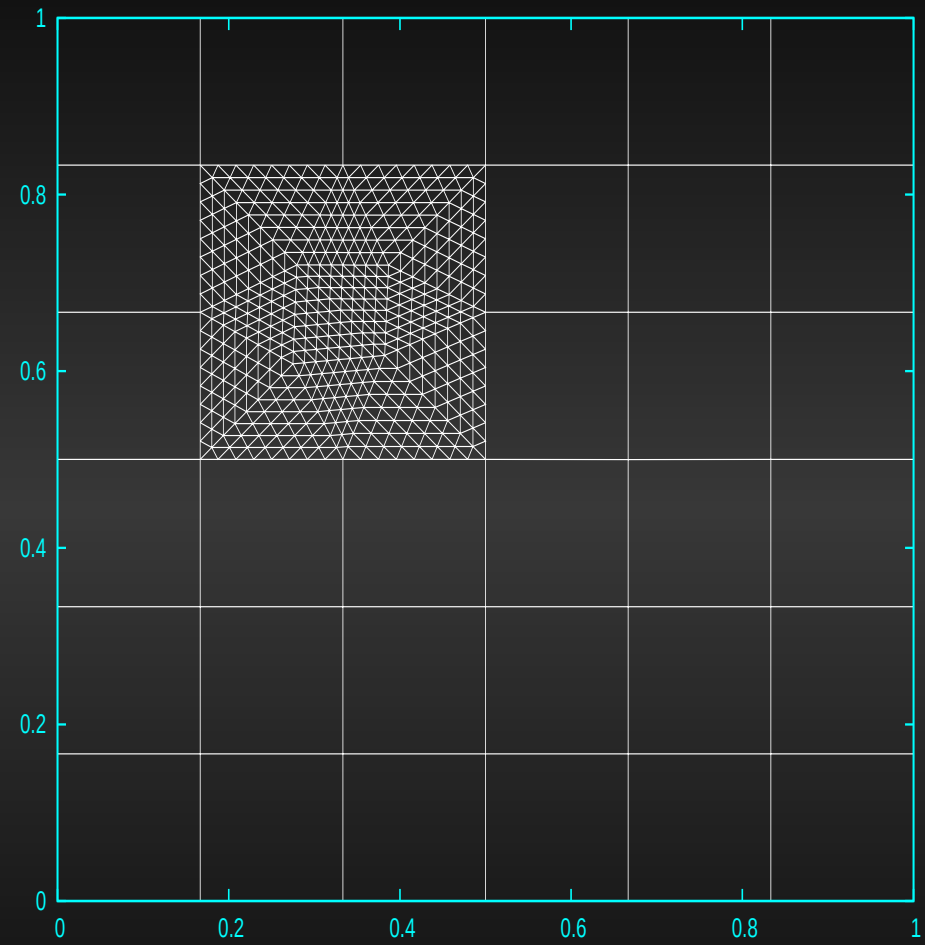

Triangles : 1024
Quadrangles : 32

Interpolation order	CPU time	# *dof*	Max L^2-error
DGTD-$\mathbb{P}_1$	71.4 s	11334	3.91×10^{-2}
DGTD-$\mathbb{P}_2$	322.8 s	22668	3.18×10^{-4}
DGTD-$\mathbb{P}_3$	918.7 s	37780	1.33×10^{-4}
DGTD-$\mathbb{P}_4$	2574.9 s	56670	5.90×10^{-5}
DGTD-$\mathbb{P}_1\mathbb{Q}_3$	16.2 s	3200	5.68×10^{-3}
DGTD-$\mathbb{P}_2\mathbb{Q}_3$	64.6 s	5888	5.84×10^{-4}
DGTD-$\mathbb{P}_3\mathbb{Q}_4$	187.5 s	9760	2.45×10^{-4}
DGTD-$\mathbb{P}_4\mathbb{Q}_4$	492.2 s	14240	1.09×10^{-4}

Comparison		$\frac{\text{CPU time}_{(a)}}{\text{CPU time}_{(b)}}$	$\frac{\text{Max } L^2\text{-error}_{(a)}}{\text{Max } L^2\text{-error}_{(b)}}$
Method (a)	Method (b)		
DGTD-$\mathbb{P}_1$	DGTD-$\mathbb{P}_1\mathbb{Q}_3$	4.41	6.88
DGTD-$\mathbb{P}_1$	DGTD-$\mathbb{P}_2\mathbb{Q}_3$	1.10	66.95
DGTD-$\mathbb{P}_2$	DGTD-$\mathbb{P}_3\mathbb{Q}_4$	1.72	1.30
DGTD-$\mathbb{P}_3$	DGTD-$\mathbb{P}_4\mathbb{Q}_4$	1.87	1.22
DGTD-$\mathbb{P}_4$	DGTD-$\mathbb{P}_4\mathbb{Q}_4$	5.23	0.54

Interpolation order	CPU time	# *dof*	Max L^2-error
DGTD-$\mathbb{P}_1$	71.4 s	11334	3.91×10^{-2}
DGTD-$\mathbb{P}_2$	322.8 s	22668	3.18×10^{-4}
DGTD-$\mathbb{P}_3$	918.7 s	37780	1.33×10^{-4}
DGTD-$\mathbb{P}_4$	2574.9 s	56670	5.90×10^{-5}
DGTD-$\mathbb{P}_1\mathbb{Q}_3$	16.2 s	3200	5.68×10^{-3}
DGTD-$\mathbb{P}_2\mathbb{Q}_3$	64.6 s	5888	5.84×10^{-4}
DGTD-$\mathbb{P}_3\mathbb{Q}_4$	187.5 s	9760	2.45×10^{-4}
DGTD-$\mathbb{P}_4\mathbb{Q}_4$	492.2 s	14240	1.09×10^{-4}

Comparison		$\frac{\text{CPU time}_{(a)}}{\text{CPU time}_{(b)}}$	$\frac{\text{Max } L^2\text{-error}_{(a)}}{\text{Max } L^2\text{-error}_{(b)}}$
Method (a)	Method (b)		
DGTD-$\mathbb{P}_1$	DGTD-$\mathbb{P}_1\mathbb{Q}_3$	4.41	6.88
DGTD-$\mathbb{P}_1$	DGTD-$\mathbb{P}_2\mathbb{Q}_3$	1.10	66.95
DGTD-$\mathbb{P}_2$	DGTD-$\mathbb{P}_3\mathbb{Q}_4$	1.72	1.30
DGTD-$\mathbb{P}_3$	DGTD-$\mathbb{P}_4\mathbb{Q}_4$	1.87	1.22
DGTD-$\mathbb{P}_4$	DGTD-$\mathbb{P}_4\mathbb{Q}_4$	5.23	0.54

Scattering of a plane wave by an airfoil profile

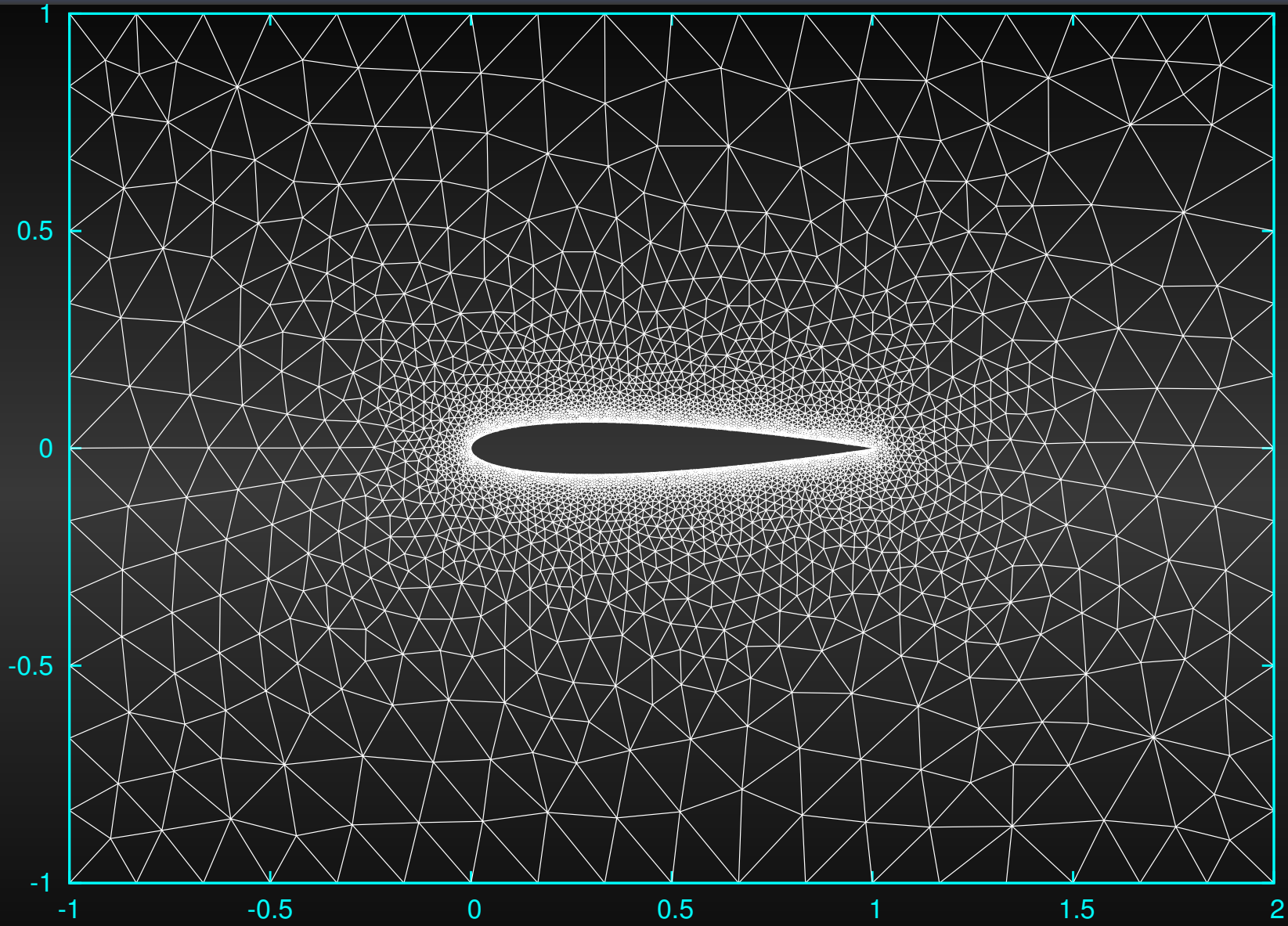

Triangles : 8444

Quadrangles : 0

Scattering of a plane wave by an airfoil profile

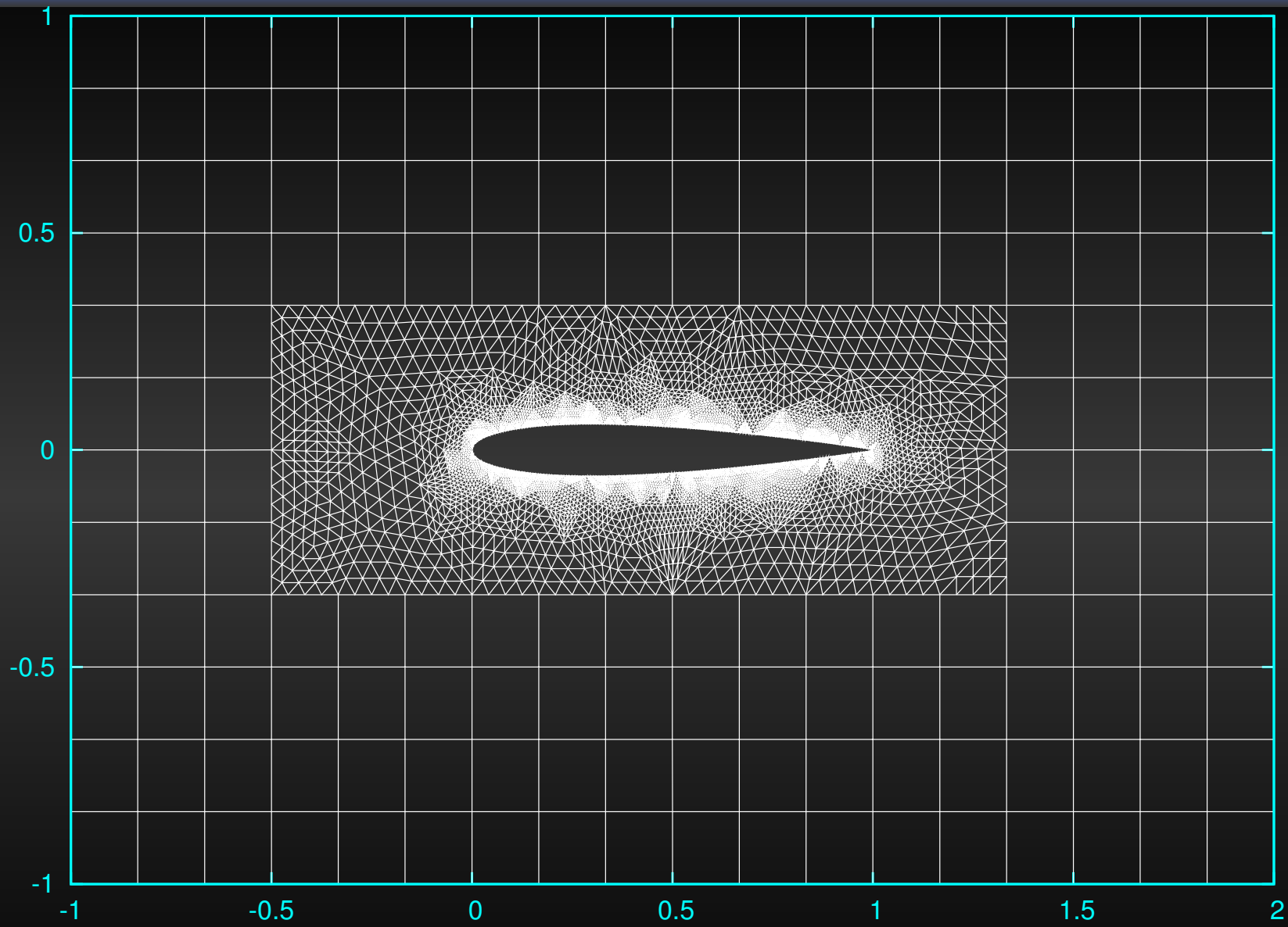

Triangles : 11584

Quadrangles : 172

- Computational domain $\Omega = [-1, 2] \times [-1, 1]$ delimited by a rectangle with the Silver-Müller absorbing boundary condition. LF2 for the other tests
- The incident field is given by :

$$\begin{cases} E_z^{\text{inc}}(x_1, x_2, t) &= \cos(\omega t - k x_1), \\ H_x^{\text{inc}}(x_1, x_2, t) &= 0, \\ H_y^{\text{inc}}(x_1, x_2, t) &= (-k/\omega)\cos(\omega t - k x_1), \end{cases}$$

with the wave vector $\mathbf{k} = (k, 0)^{\mathrm{T}}$ where $k = \omega/c$ (c the speed of light in vacuum) and $\omega = 2\pi f$ where $f = 600$ MHz denotes the frequency

Interpolation order	CPU time	# *dof*
$\mathbb{P}_4$	1201.9 s	126660
$\mathbb{P}_2\mathbb{Q}_4$	152.2 s	73804
$\mathbb{P}_3\mathbb{Q}_4$	437.7 s	120140

Comparison		$\frac{\text{CPU time}_{(a)}}{\text{CPU time}_{(b)}}$	$\frac{\#\ dof_{(a)}}{\#\ dof_{(b)}}$
Method (a)	Method (b)		
DGTD-$\mathbb{P}_4$	DGTD-$\mathbb{P}_2\mathbb{Q}_4$	7.90	1.71
DGTD-$\mathbb{P}_4$	DGTD-$\mathbb{P}_3\mathbb{Q}_4$	2.75	1.05

- Computational domain $\Omega = [-1, 2] \times [-1, 1]$ delimited by a rectangle with the Silver-Müller absorbing boundary condition. LF2 for the other tests
- The incident field is given by :

$$\begin{cases} E_z^{\text{inc}}(x_1, x_2, t) &= \cos(\omega t - k x_1), \\ H_x^{\text{inc}}(x_1, x_2, t) &= 0, \\ H_y^{\text{inc}}(x_1, x_2, t) &= (-k/\omega)\cos(\omega t - k x_1), \end{cases}$$

with the wave vector $\mathbf{k} = (k, 0)^{\mathrm{T}}$ where $k = \omega/c$ (c the speed of light in vacuum) and $\omega = 2\pi f$ where $f = 600$ MHz denotes the frequency

Interpolation order	CPU time	# *dof*
$\mathbb{P}_4$	1201.9 s	126660
$\mathbb{P}_2\mathbb{Q}_4$	152.2 s	73804
$\mathbb{P}_3\mathbb{Q}_4$	437.7 s	120140

Comparison		$\frac{\text{CPU time}_{(a)}}{\text{CPU time}_{(b)}}$	$\frac{\#\ dof_{(a)}}{\#\ dof_{(b)}}$
Method (a)	Method (b)		
DGTD-$\mathbb{P}_4$	DGTD-$\mathbb{P}_2\mathbb{Q}_4$	7.90	1.71
DGTD-$\mathbb{P}_4$	DGTD-$\mathbb{P}_3\mathbb{Q}_4$	2.75	1.05

Time evolution of E_z component at points $(-0.1; 0.0)$ and $(1.6; -0.6)$:

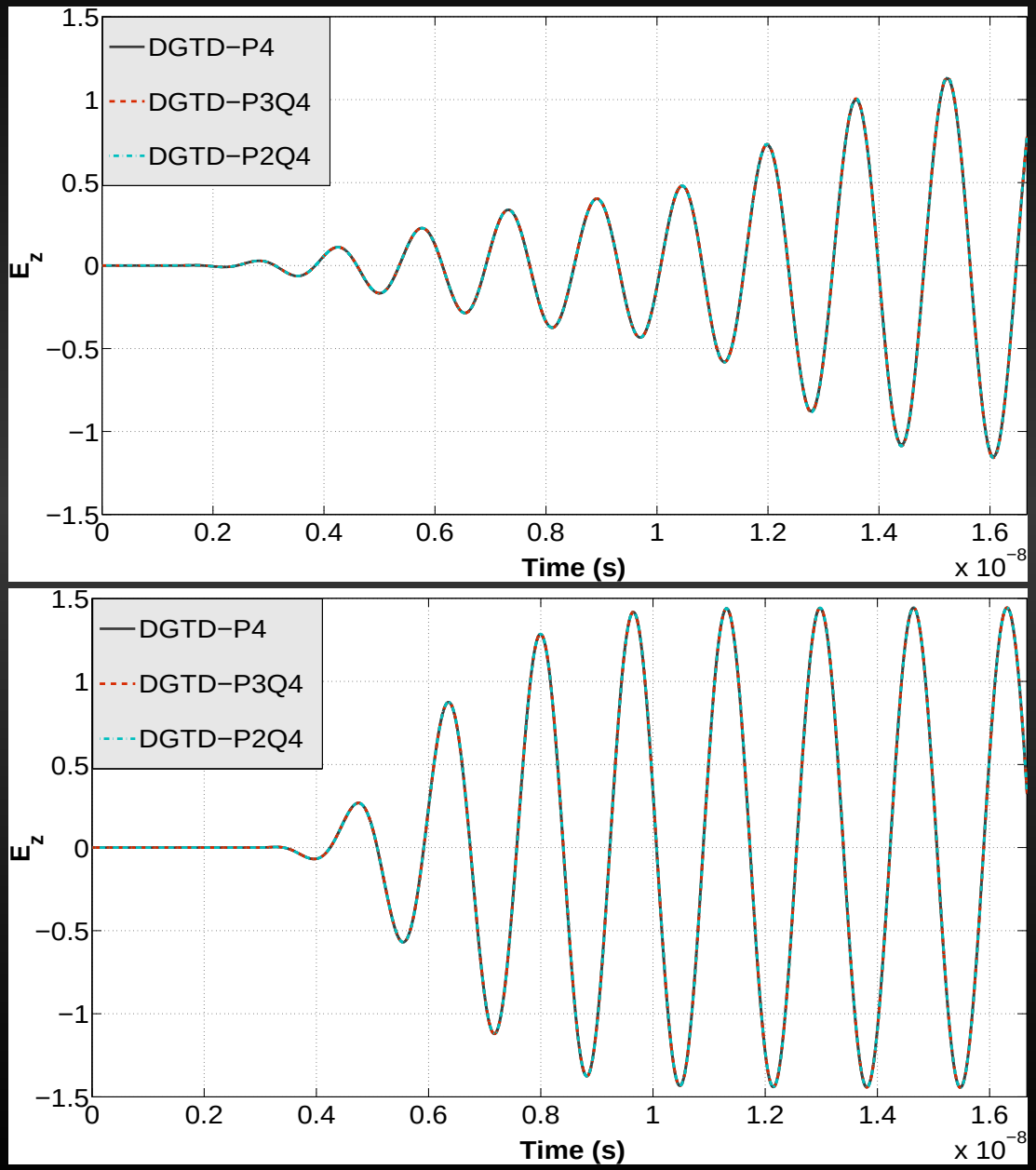

Contour lines of discrete Fourier transform of E_z and H_y components for DGTD-$\mathbb{P}_4$:

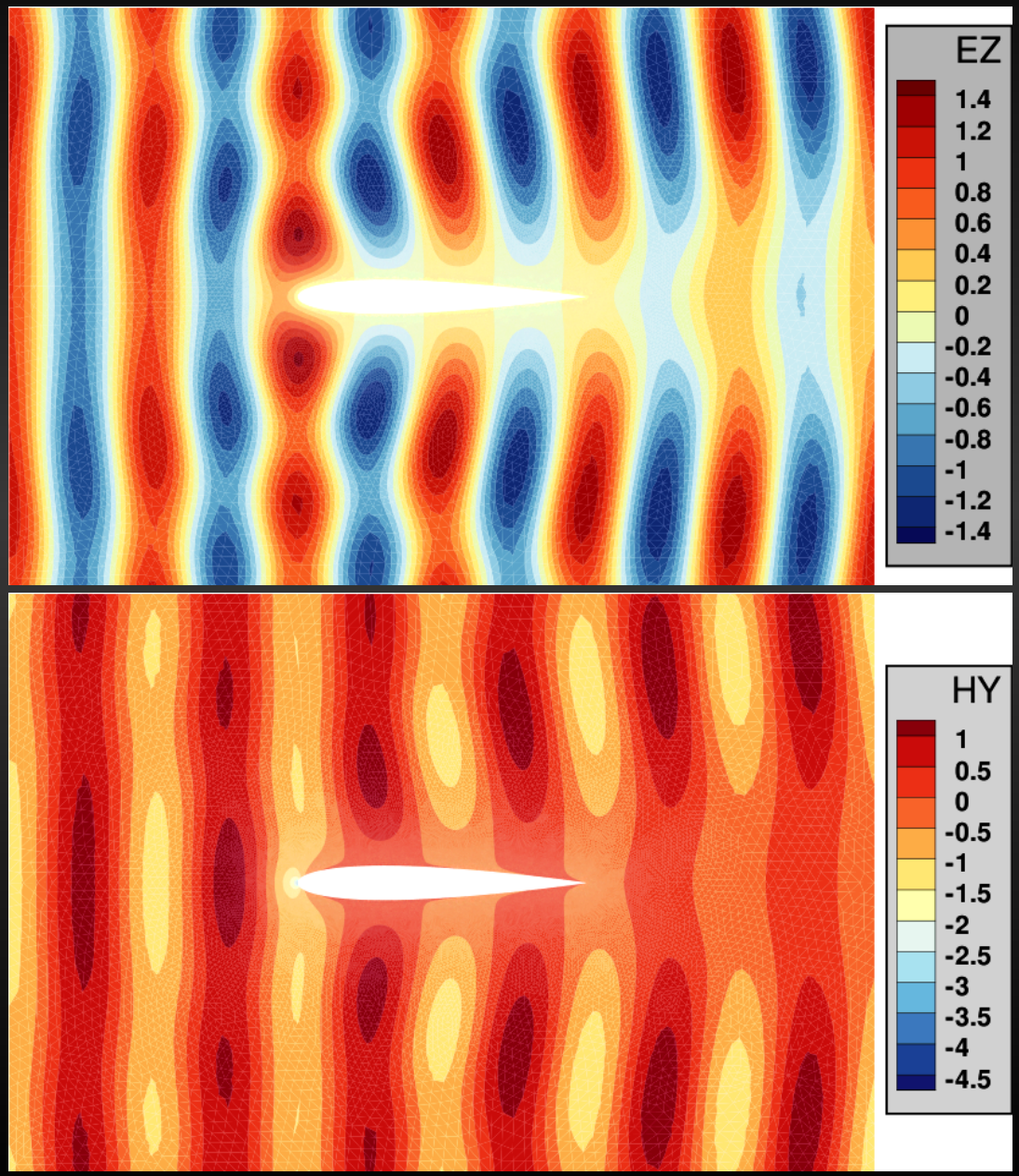

Contour lines of discrete Fourier transform of E_z and H_y components for DGTD-$\mathbb{P}_2\mathbb{Q}_4$:

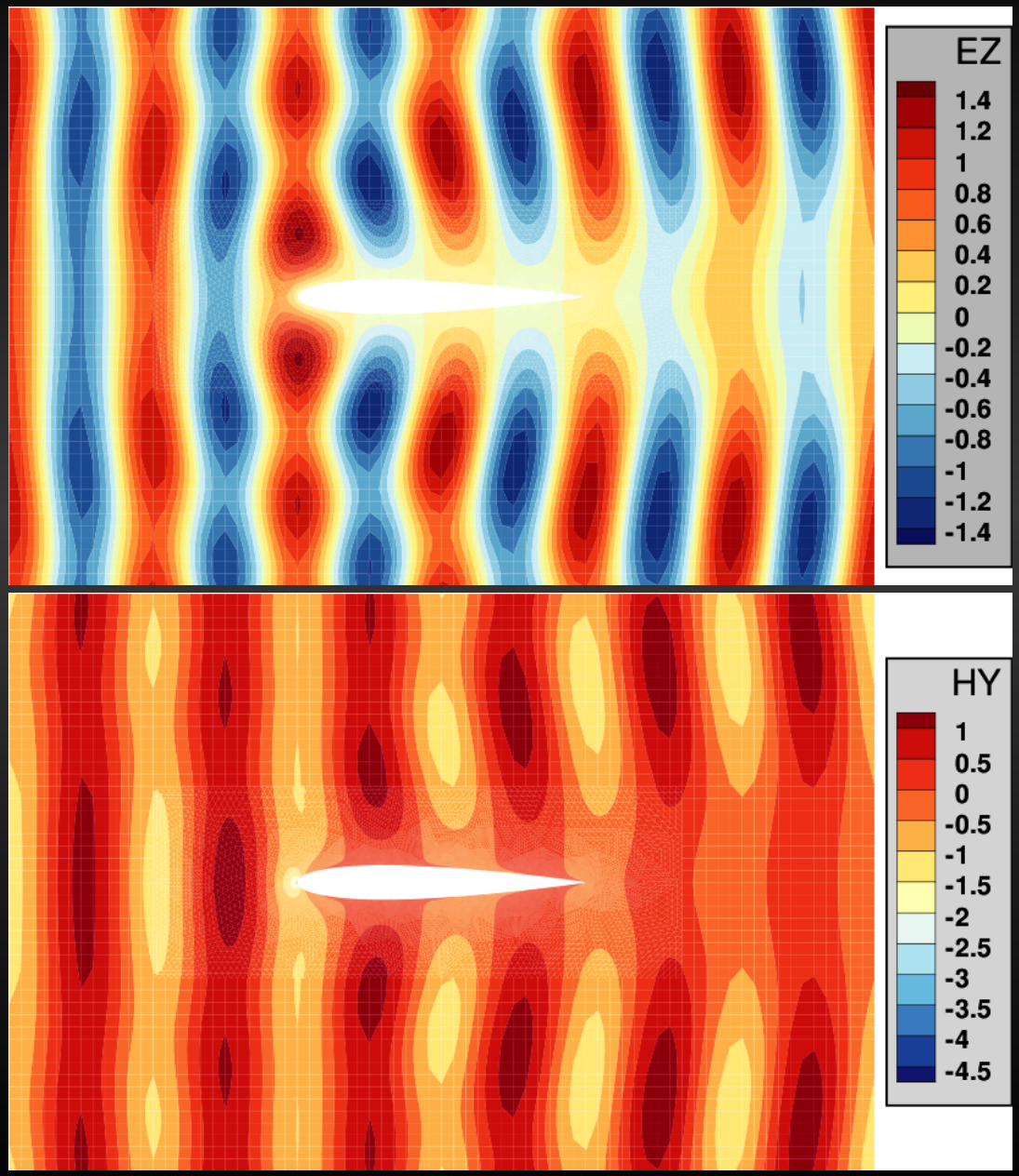

Contour lines of discrete Fourier transform of E_z and H_y components for DGTD-$\mathbb{P}_3\mathbb{Q}_4$:

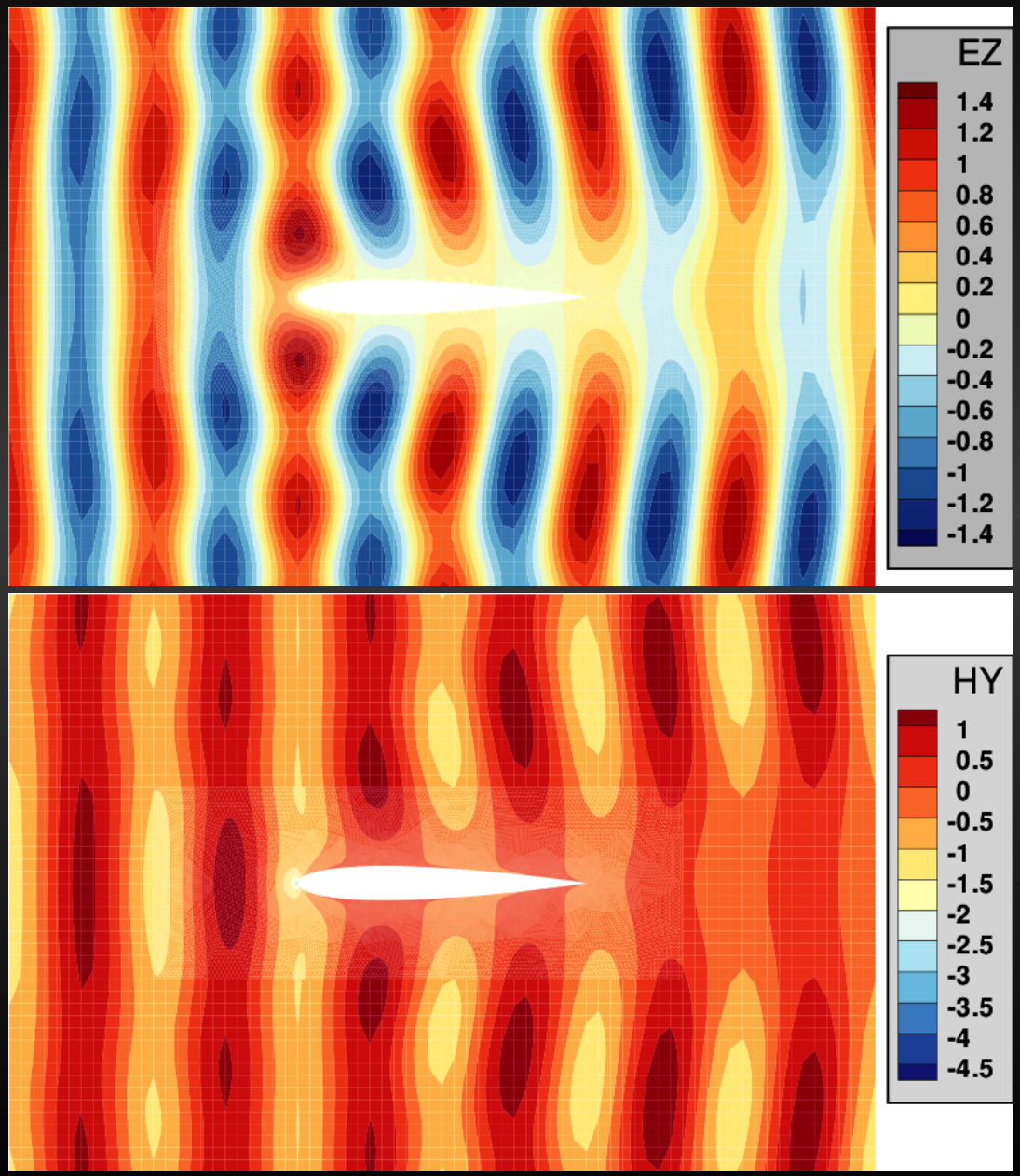

Scattering of a plane wave by a dielectric disk

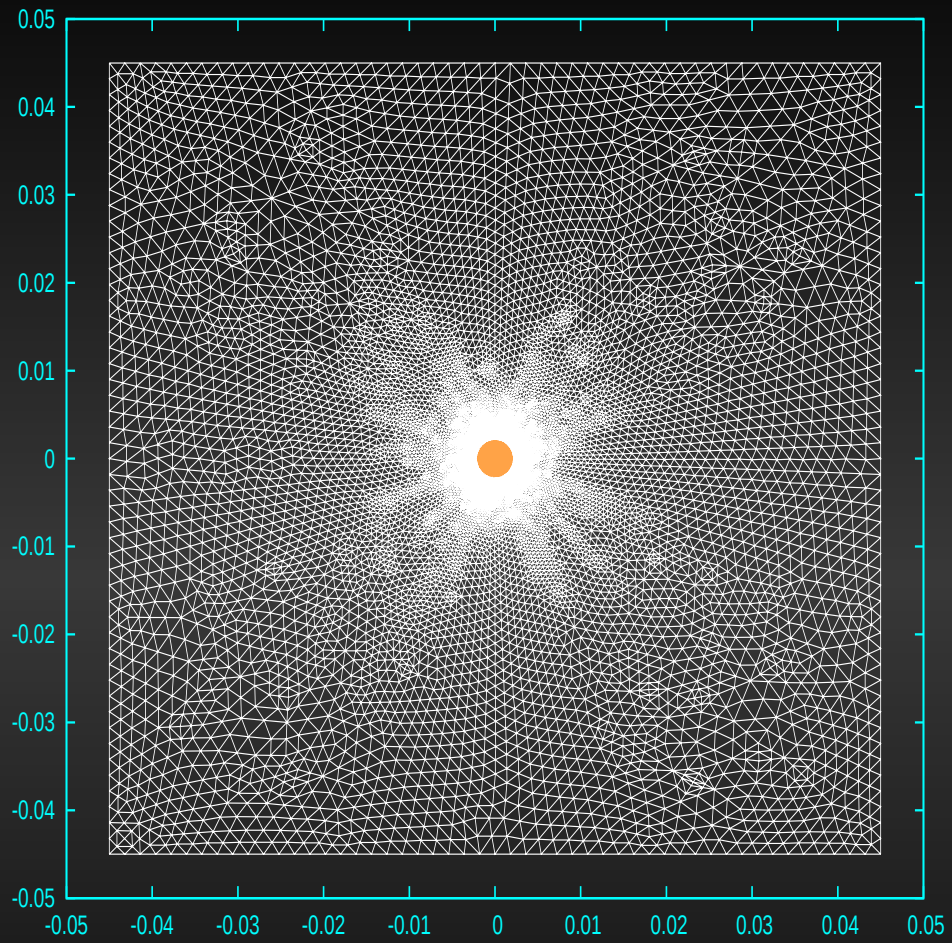

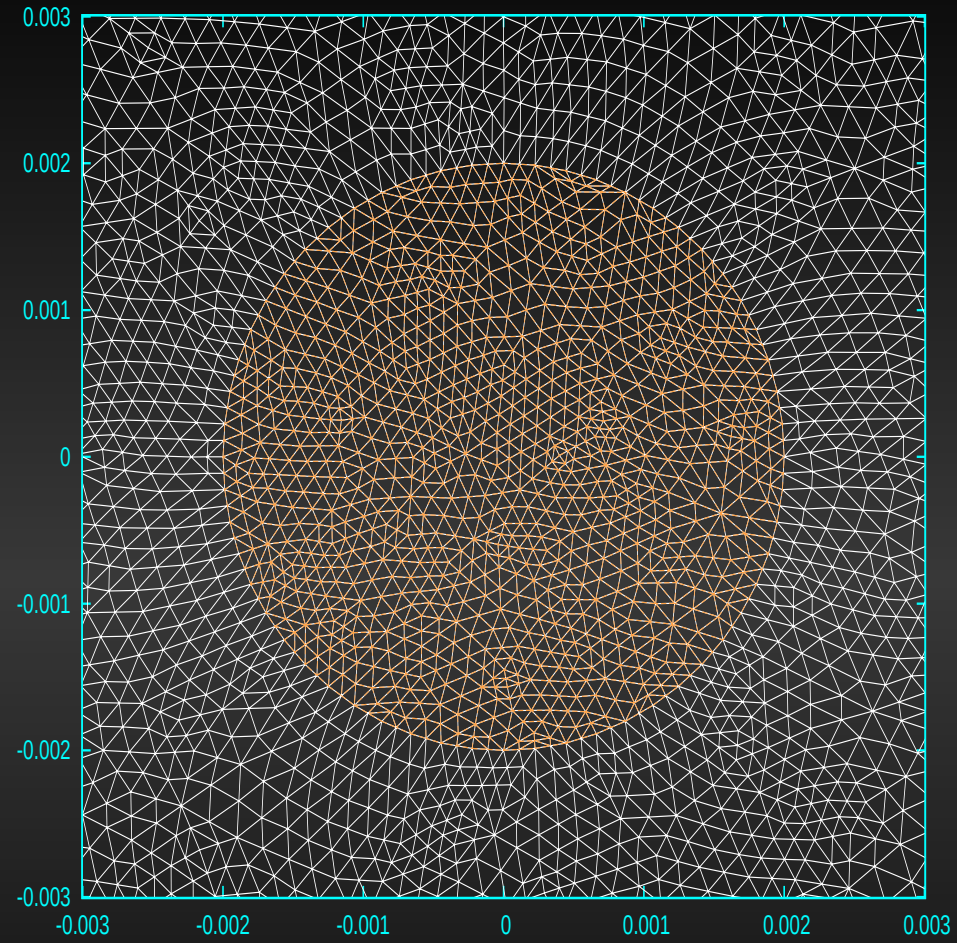

Triangles : 22216

Quadrangles : 0

Scattering of a plane wave by a dielectric disk

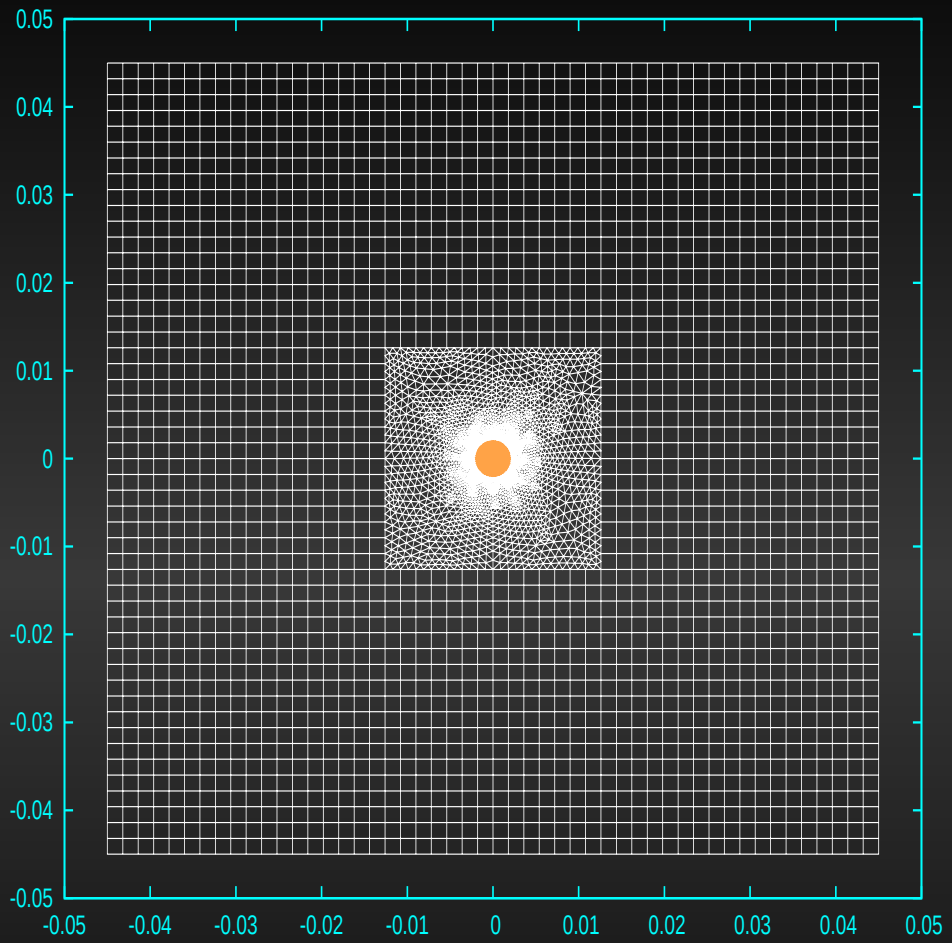

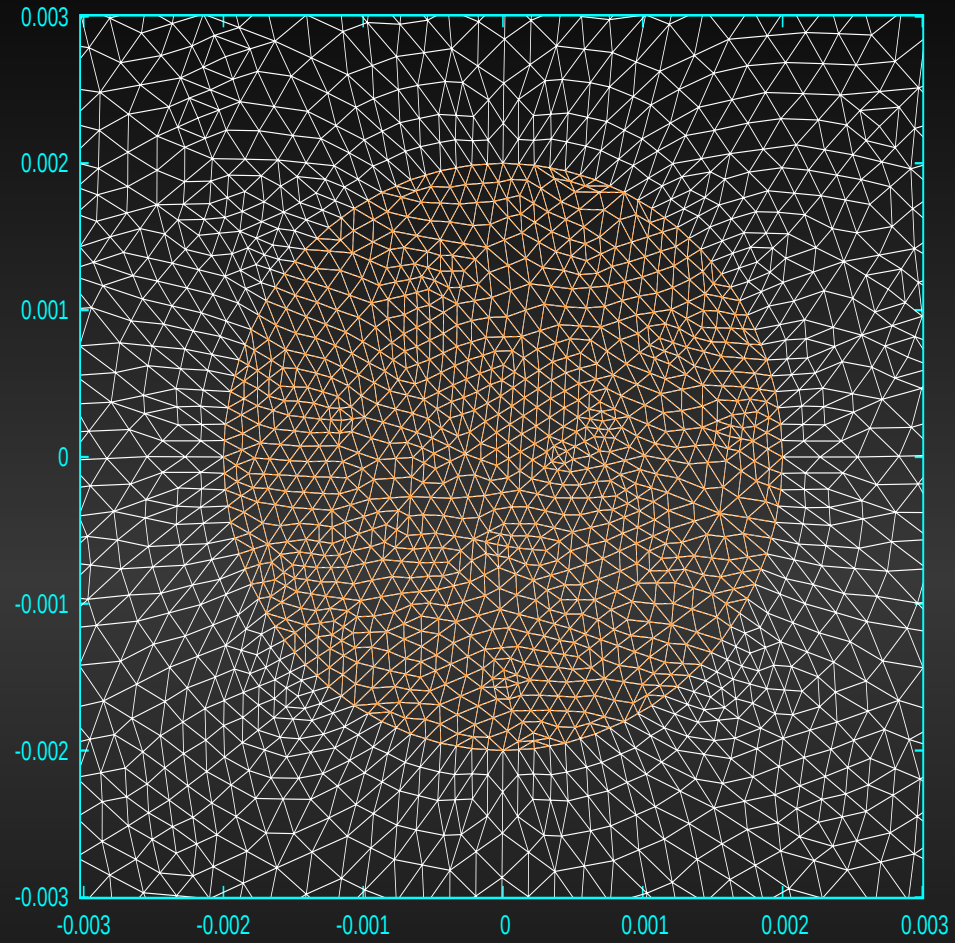

Triangles : 7128

Quadrangles : 2304

- $\Omega = [-0.045, 0.045] \times [-0.045, 0.045]$, Silver-Müller boundary condition
- Heterogeneous media. Radius of the disk : 0.002 m. Outside the disk : $\varepsilon_1 = \mu_1 = 1$. Inside the disk : $\varepsilon_2 = 7$ and $\mu_2 = 1$. Frequency $f = 30$ GHz.
- E_z component of the exact solution :

$$E_z(r,\theta,t) = e^{i\omega t} \begin{cases} \sum_{n=-\infty}^{\infty} C_n^{\text{tot}} J_n(\kappa_2 r) e^{in\theta}, & r \leq R, \\ \sum_{n=-\infty}^{\infty} (i^{-n} J_n(\kappa_1 r) + C_n^{\text{scat}} H_n^{(2)}(\kappa_1 r)) e^{in\theta}, & r > R, \end{cases}$$

where $\kappa_1 = \omega\sqrt{\varepsilon_1\mu_1}$, $\kappa_2 = \omega\sqrt{\varepsilon_2\mu_2}$, (r,θ) the polar coordinates, J_n the Bessel functions of the first kind, $H_n^{(2)}$ Hankel functions of the second type. C_n^{tot} and C_n^{scat} are the expansion coefficients for the total filed interior to the disk, and for the scattered field. Reminder : $E_z(r,\theta,t) = E_z(x_1,x_2,t)$.

Interpolation order	CPU time	# *dof*	Fourier L^2-error
DGTD-$\mathbb{P}_2$	391.1 s	133296	2.40×10^{-2}
DGTD-$\mathbb{P}_3$	1351.0 s	222160	6.21×10^{-3}
DGTD-$\mathbb{P}_2\mathbb{Q}_2$	165.6 s	63504	1.86×10^{-2}
DGTD-$\mathbb{P}_3\mathbb{Q}_2$	458.7 s	92016	4.88×10^{-3}

- $\Omega = [-0.045, 0.045] \times [-0.045, 0.045]$, Silver-Müller boundary condition
- Heterogeneous media. Radius of the disk : 0.002 m. Outside the disk : $\varepsilon_1 = \mu_1 = 1$. Inside the disk : $\varepsilon_2 = 7$ and $\mu_2 = 1$. Frequency $f = 30$ GHz.
- E_z component of the exact solution :

$$E_z(r,\theta,t) = e^{\mathrm{i}\omega t} \begin{cases} \sum_{n=-\infty}^{\infty} C_n^{\mathrm{tot}} J_n(\kappa_2 r) e^{\mathrm{i}n\theta}, & r \leq R, \\ \sum_{n=-\infty}^{\infty} (\mathrm{i}^{-n} J_n(\kappa_1 r) + C_n^{\mathrm{scat}} H_n^{(2)}(\kappa_1 r)) e^{\mathrm{i}n\theta}, & r > R, \end{cases}$$

where $\kappa_1 = \omega\sqrt{\varepsilon_1\mu_1}$, $\kappa_2 = \omega\sqrt{\varepsilon_2\mu_2}$, (r,θ) the polar coordinates, J_n the Bessel functions of the first kind, $H_n^{(2)}$ Hankel functions of the second type. C_n^{tot} and C_n^{scat} are the expansion coefficients for the total filed interior to the disk, and for the scattered field. Reminder : $E_z(r,\theta,t) = E_z(x_1,x_2,t)$.

Interpolation order	CPU time	# *dof*	Fourier L^2-error
DGTD-$\mathbb{P}_2$	391.1 s	133296	2.40×10^{-2}
DGTD-$\mathbb{P}_3$	1351.0 s	222160	6.21×10^{-3}
DGTD-$\mathbb{P}_2\mathbb{Q}_2$	165.6 s	63504	1.86×10^{-2}
DGTD-$\mathbb{P}_3\mathbb{Q}_2$	458.7 s	92016	4.88×10^{-3}

- $\Omega = [-0.045, 0.045] \times [-0.045, 0.045]$, Silver-Müller boundary condition
- Heterogeneous media. Radius of the disk : 0.002 m. Outside the disk : $\varepsilon_1 = \mu_1 = 1$. Inside the disk : $\varepsilon_2 = 7$ and $\mu_2 = 1$. Frequency $f = 30$ GHz.
- E_z component of the exact solution :

$$E_z(r,\theta,t) = e^{i\omega t} \begin{cases} \sum_{n=-\infty}^{\infty} C_n^{\text{tot}} J_n(\kappa_2 r) e^{in\theta}, & r \leq R, \\ \sum_{n=-\infty}^{\infty} (i^{-n} J_n(\kappa_1 r) + C_n^{\text{scat}} H_n^{(2)}(\kappa_1 r)) e^{in\theta}, & r > R, \end{cases}$$

where $\kappa_1 = \omega\sqrt{\varepsilon_1\mu_1}$, $\kappa_2 = \omega\sqrt{\varepsilon_2\mu_2}$, (r,θ) the polar coordinates, J_n the Bessel functions of the first kind, $H_n^{(2)}$ Hankel functions of the second type. C_n^{tot} and C_n^{scat} are the expansion coefficients for the total filed interior to the disk, and for the scattered field. Reminder : $E_z(r,\theta,t) = E_z(x_1,x_2,t)$.

Interpolation order	CPU time	# *dof*	Fourier L^2-error
DGTD-$\mathbb{P}_2$	391.1 s	133296	2.40×10^{-2}
DGTD-$\mathbb{P}_3$	1351.0 s	222160	6.21×10^{-3}
DGTD-$\mathbb{P}_2\mathbb{Q}_2$	165.6 s	63504	1.86×10^{-2}
DGTD-$\mathbb{P}_3\mathbb{Q}_2$	458.7 s	92016	4.88×10^{-3}

1D distribution of discrete Fourier transform of H_y component along $x_2 = 0.0$:

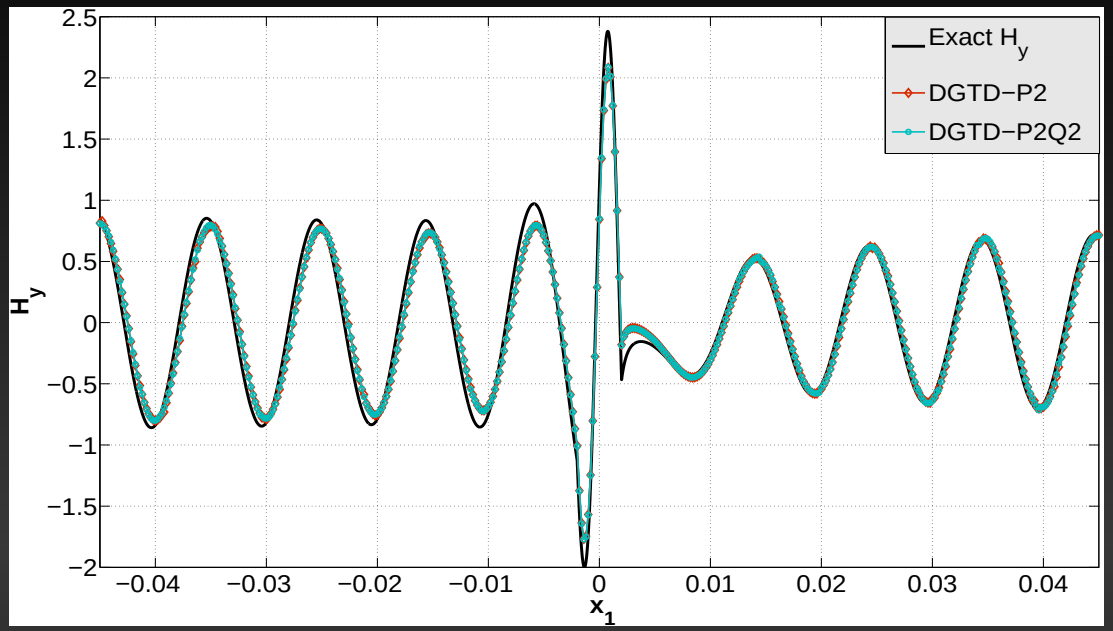

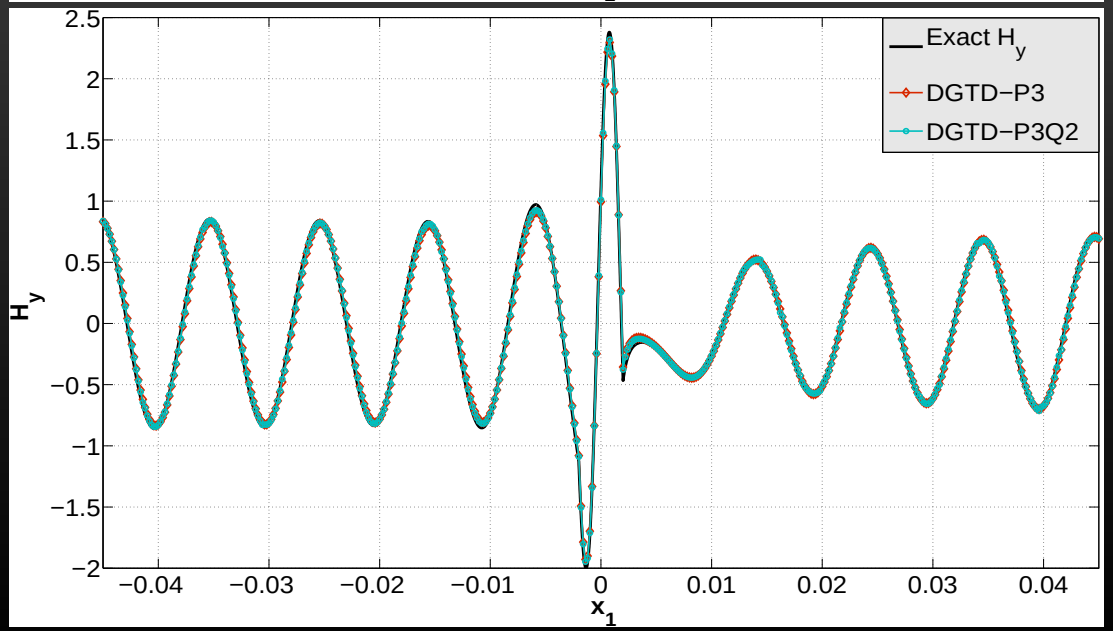

Contour lines of discrete Fourier transform of E_z component for the exact solution :

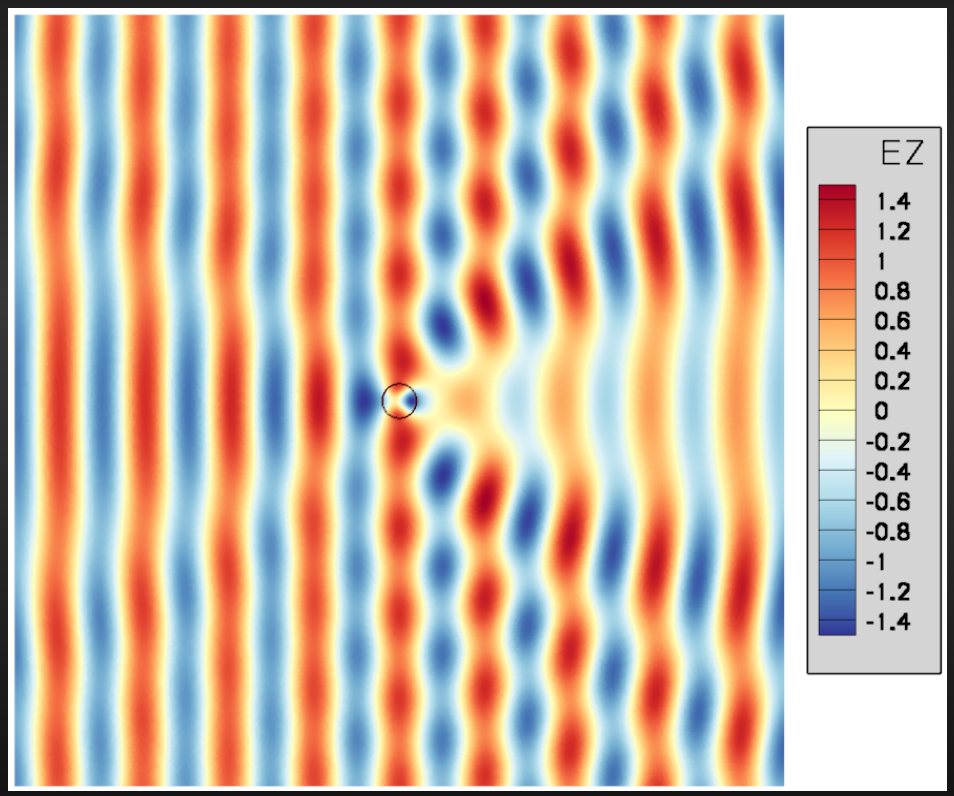

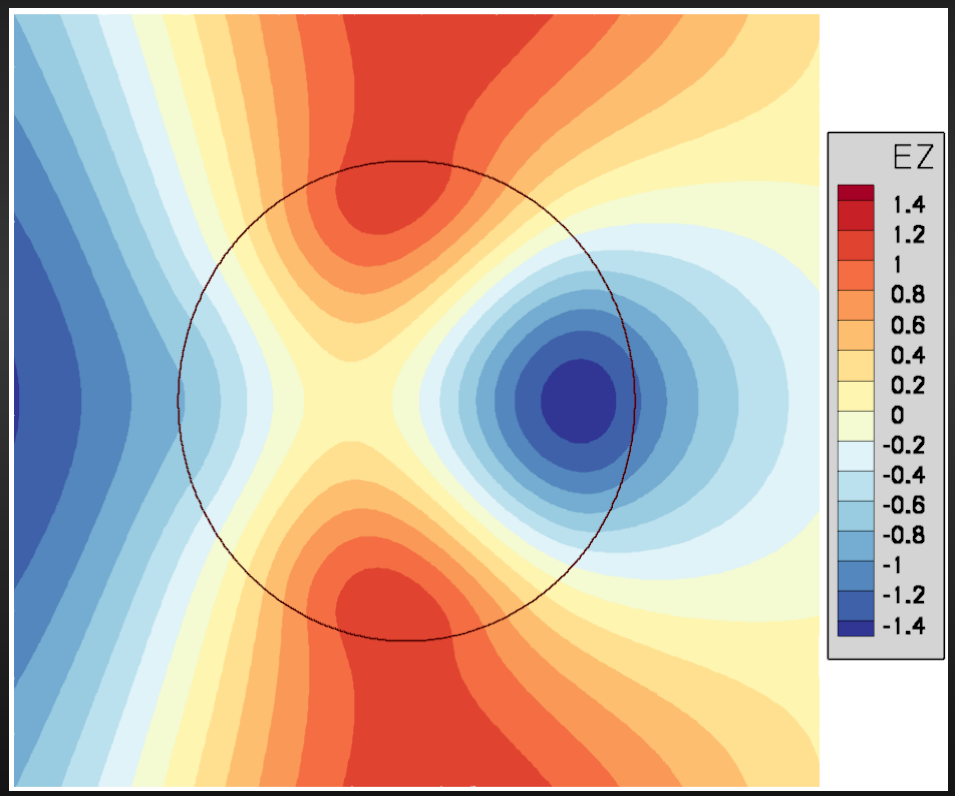

Contour lines of discrete Fourier transform of E_z component for the DGTD-$\mathbb{P}_3\mathbb{Q}_2$ method :

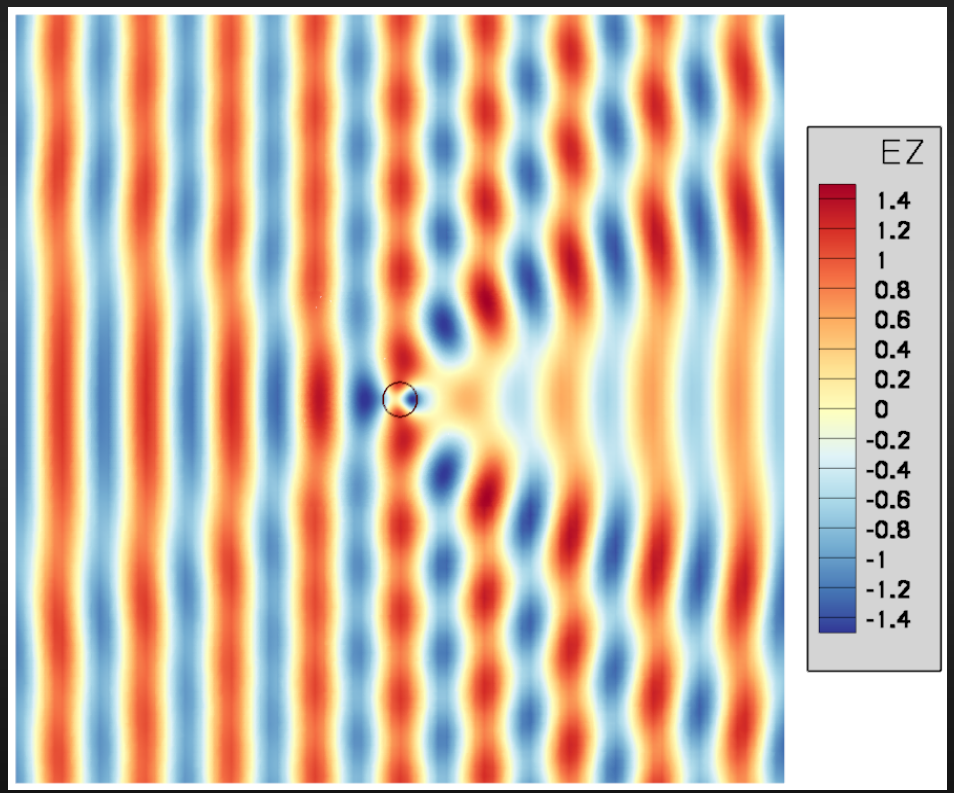

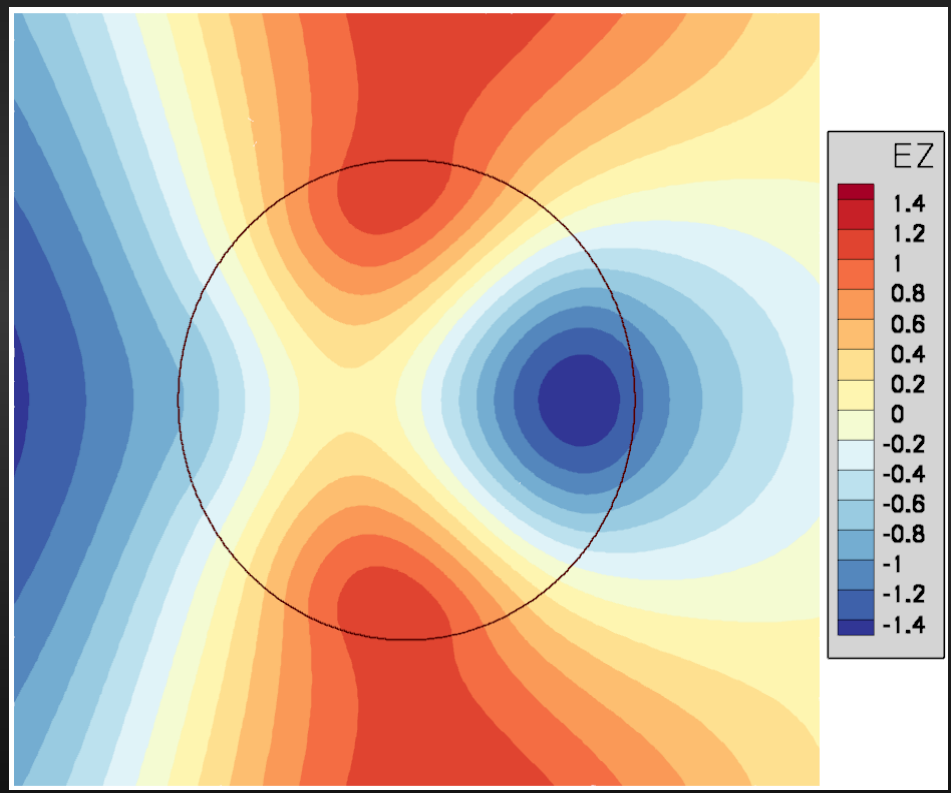

Outline

- Evolution of the (1,1,1) mode in a PEC cubic cavity, $\Omega = [0,1]^3$
- Metallic boundary condition, $f = 260$ MHz
- The exact solution is ($\omega = 2\pi f$) :

$$\begin{cases} H_x(x_1,x_2,t) &= -(\pi/\omega)\sin(\pi x_1)\cos(\pi x_2)\cos(\pi x_3)\sin(\omega t), \\ H_y(x_1,x_2,t) &= (2\pi/\omega)\cos(\pi x_1)\sin(\pi x_2)\cos(\pi x_3)\sin(\omega t), \\ H_z(x_1,x_2,t) &= -(\pi/\omega)\cos(\pi x_1)\cos(\pi x_2)\sin(\pi x_3)\sin(\omega t), \\ E_x(x_1,x_2,t) &= -\cos(\pi x_1)\sin(\pi x_2)\sin(\pi x_3)\sin(\omega t), \\ E_y(x_1,x_2,t) &= 0, \\ E_z(x_1,x_2,t) &= \sin(\pi x_1)\sin(\pi x_2)\cos(\pi x_3)\cos(\omega t). \end{cases}$$

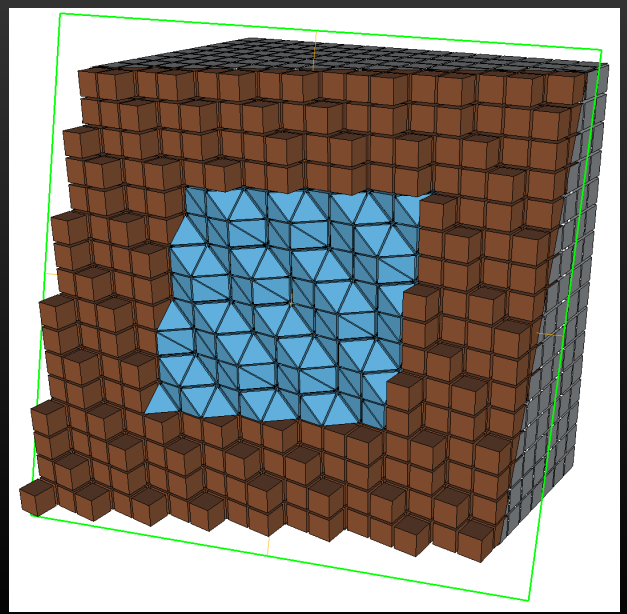

Numerical h-wise convergence for the DGTD-$\mathbb{P}_p\mathbb{Q}_k$ method :

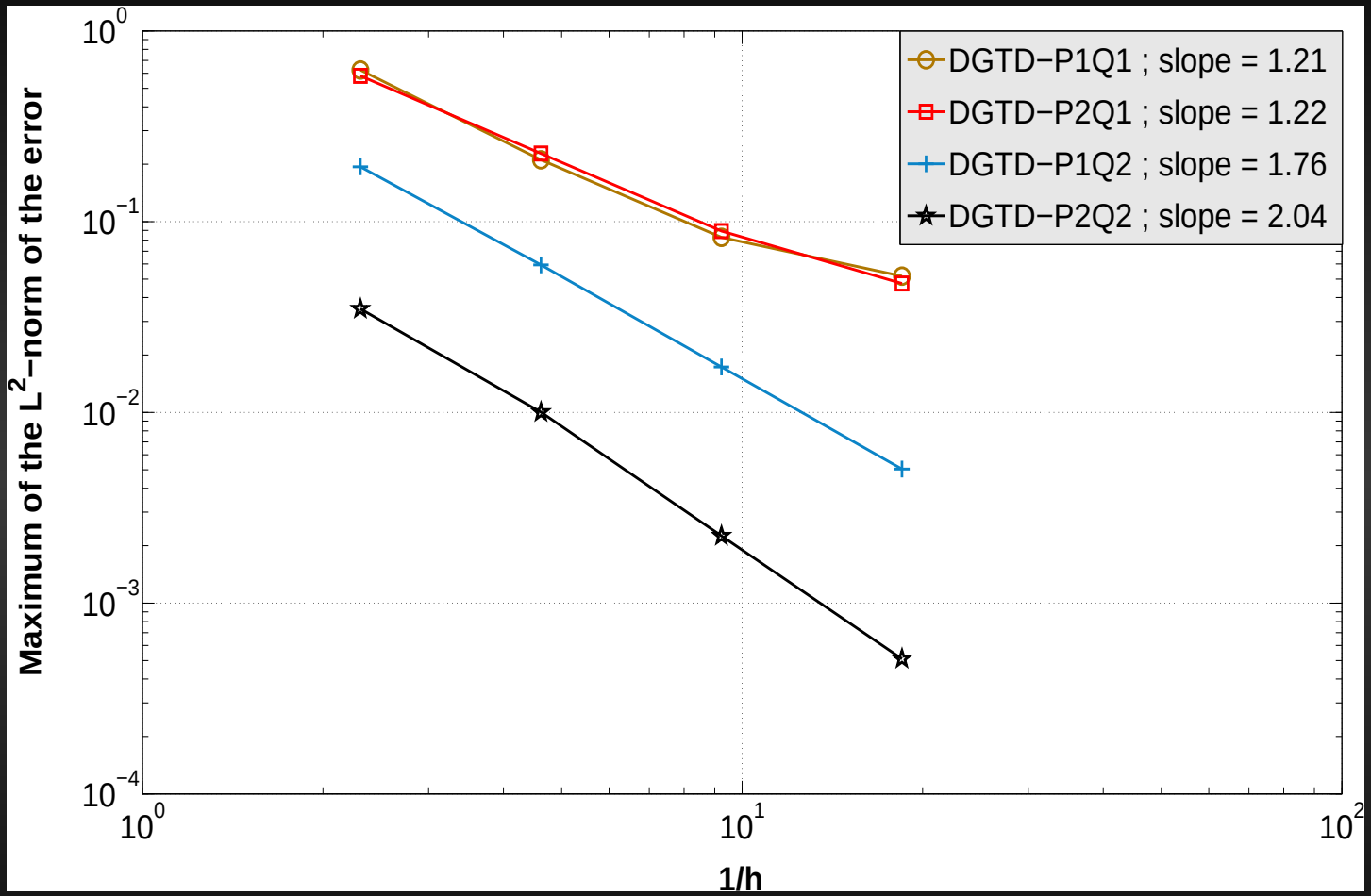

- Numerical validation of convergence in h. Stable method.
- Right orders of convergence.

Eigenmode in a unitary PEC cubic cavity

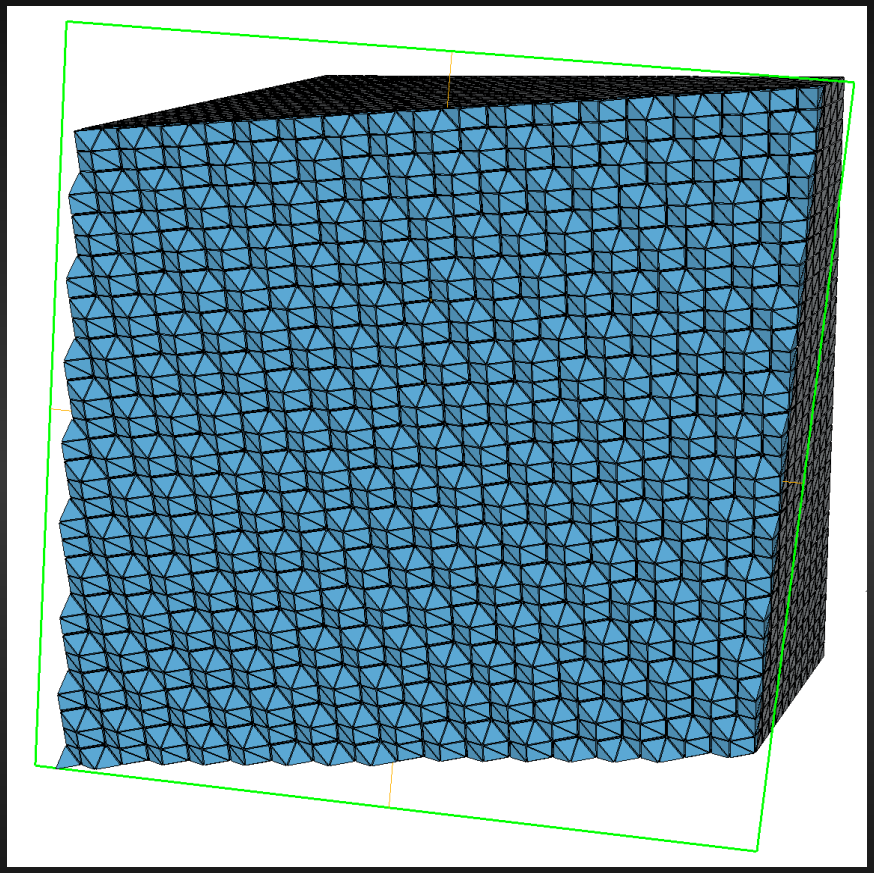

Tetrahedra : 196608
Hexahedra : 0

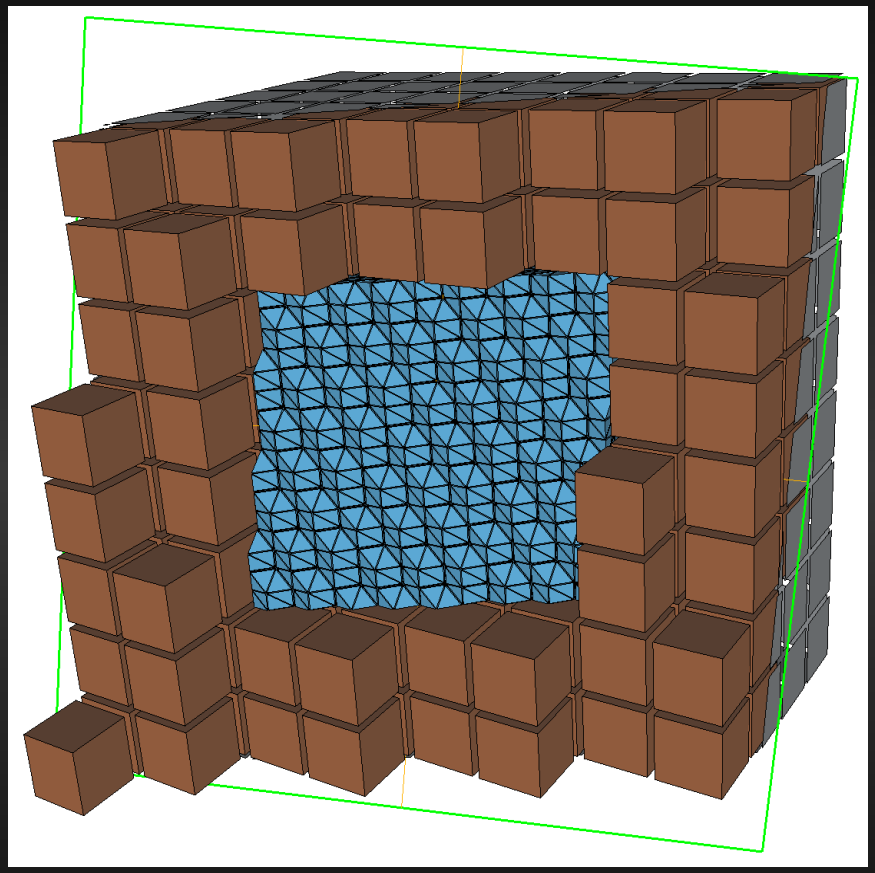

Tetrahedra : 24576
Hexahedra : 448

Interpolation order	CPU time	# *dof*	Max L^2-error
DGTD-$\mathbb{P}_1$	26 min 9 s	786432	8.37×10^{-3}
DGTD-$\mathbb{P}_2$	150 min 56 s	1966080	5.50×10^{-4}
DGTD-$\mathbb{P}_1\mathbb{Q}_1$	3 min 33 s	101888	2.19×10^{-1}
DGTD-$\mathbb{P}_1\mathbb{Q}_2$	4 min 37 s	110400	4.23×10^{-3}
DGTD-$\mathbb{P}_2\mathbb{Q}_1$	20 min 23 s	249344	2.30×10^{-1}
DGTD-$\mathbb{P}_2\mathbb{Q}_2$	22 min 55 s	257856	1.92×10^{-3}

Comparison		$\frac{\text{CPU time}_{(a)}}{\text{CPU time}_{(b)}}$	$\frac{\text{Max } L^2\text{-error}_{(a)}}{\text{Max } L^2\text{-error}_{(b)}}$
Method (a)	Method (b)		
DGTD-$\mathbb{P}_1$	DGTD-$\mathbb{P}_1\mathbb{Q}_2$	5.66	1.98
DGTD-$\mathbb{P}_1$	DGTD-$\mathbb{P}_2\mathbb{Q}_2$	1.14	4.36
DGTD-$\mathbb{P}_2$	DGTD-$\mathbb{P}_2\mathbb{Q}_2$	6.59	0.29

Interpolation order	CPU time	# *dof*	Max L^2-error
DGTD-$\mathbb{P}_1$	26 min 9 s	786432	8.37×10^{-3}
DGTD-$\mathbb{P}_2$	150 min 56 s	1966080	5.50×10^{-4}
DGTD-$\mathbb{P}_1\mathbb{Q}_1$	3 min 33 s	101888	2.19×10^{-1}
DGTD-$\mathbb{P}_1\mathbb{Q}_2$	4 min 37 s	110400	4.23×10^{-3}
DGTD-$\mathbb{P}_2\mathbb{Q}_1$	20 min 23 s	249344	2.30×10^{-1}
DGTD-$\mathbb{P}_2\mathbb{Q}_2$	22 min 55 s	257856	1.92×10^{-3}

Comparison		$\frac{\text{CPU time}_{(a)}}{\text{CPU time}_{(b)}}$	$\frac{\text{Max } L^2\text{-error}_{(a)}}{\text{Max } L^2\text{-error}_{(b)}}$
Method (a)	Method (b)		
DGTD-$\mathbb{P}_1$	DGTD-$\mathbb{P}_1\mathbb{Q}_2$	5.66	1.98
DGTD-$\mathbb{P}_1$	DGTD-$\mathbb{P}_2\mathbb{Q}_2$	1.14	4.36
DGTD-$\mathbb{P}_2$	DGTD-$\mathbb{P}_2\mathbb{Q}_2$	6.59	0.29

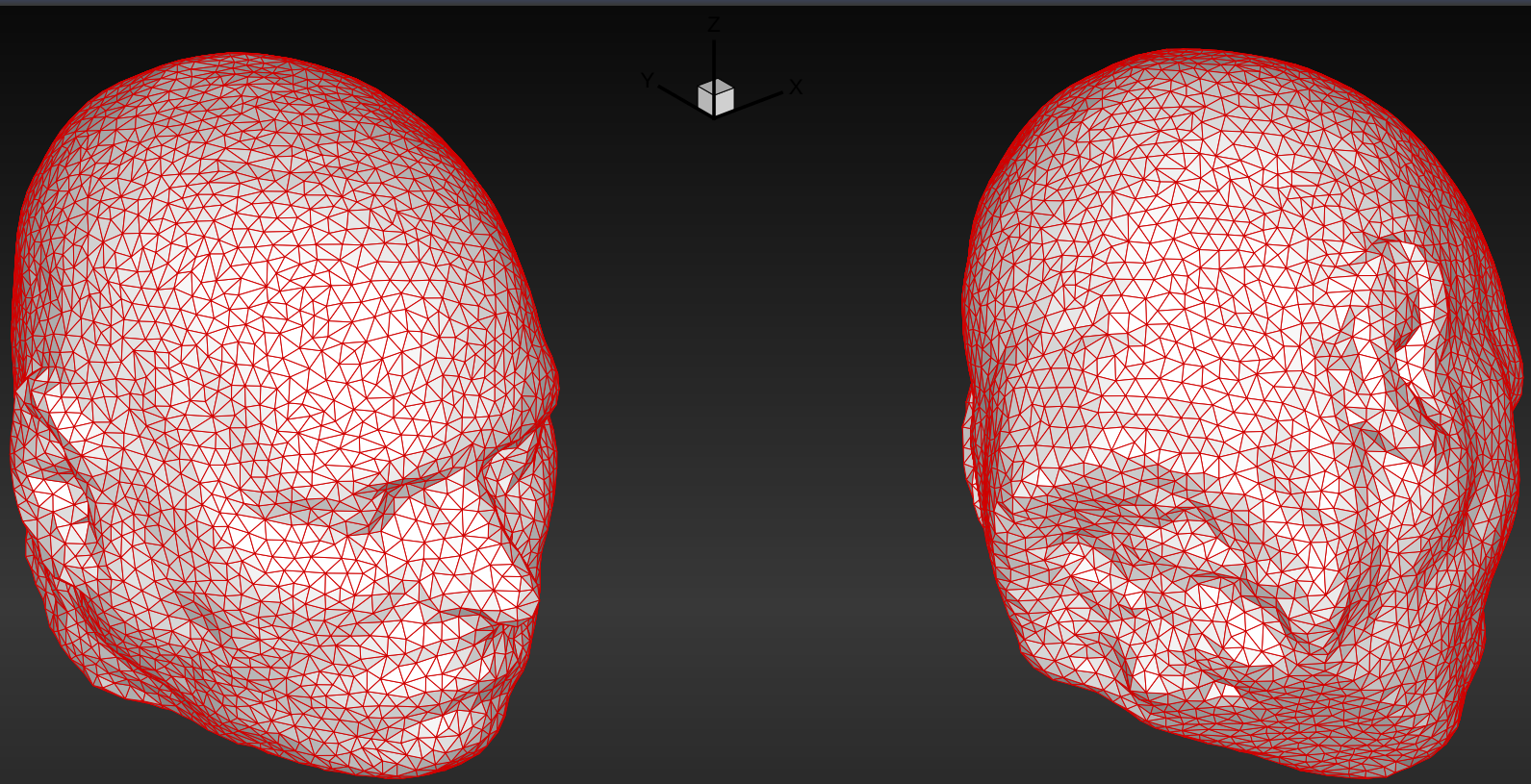

Propagation medium	ε_r	σ
Air (or vacuum)	1.00	0
Skin	43.85	1.23
Skull	15.56	0.43
Cerebrospinal fluid	67.20	2.92
Brain	43.55	1.15

Propagation in a heterogeneous human head model

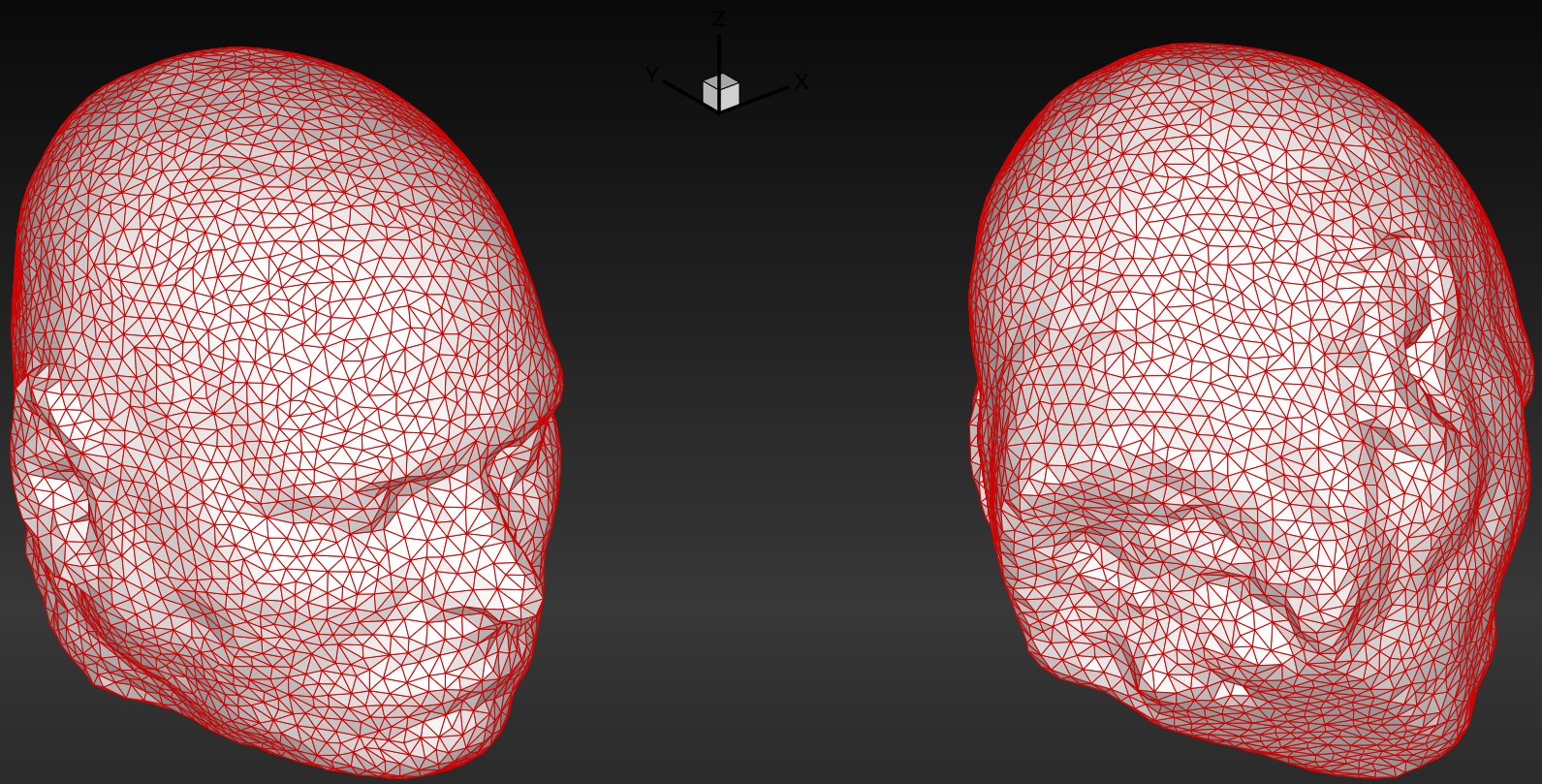

Propagation medium	ε_r	σ
Air (or vacuum)	1.00	0
Skin	43.85	1.23
Skull	15.56	0.43
Cerebrospinal fluid	67.20	2.92
Brain	43.55	1.15

Propagation in a heterogeneous human head model

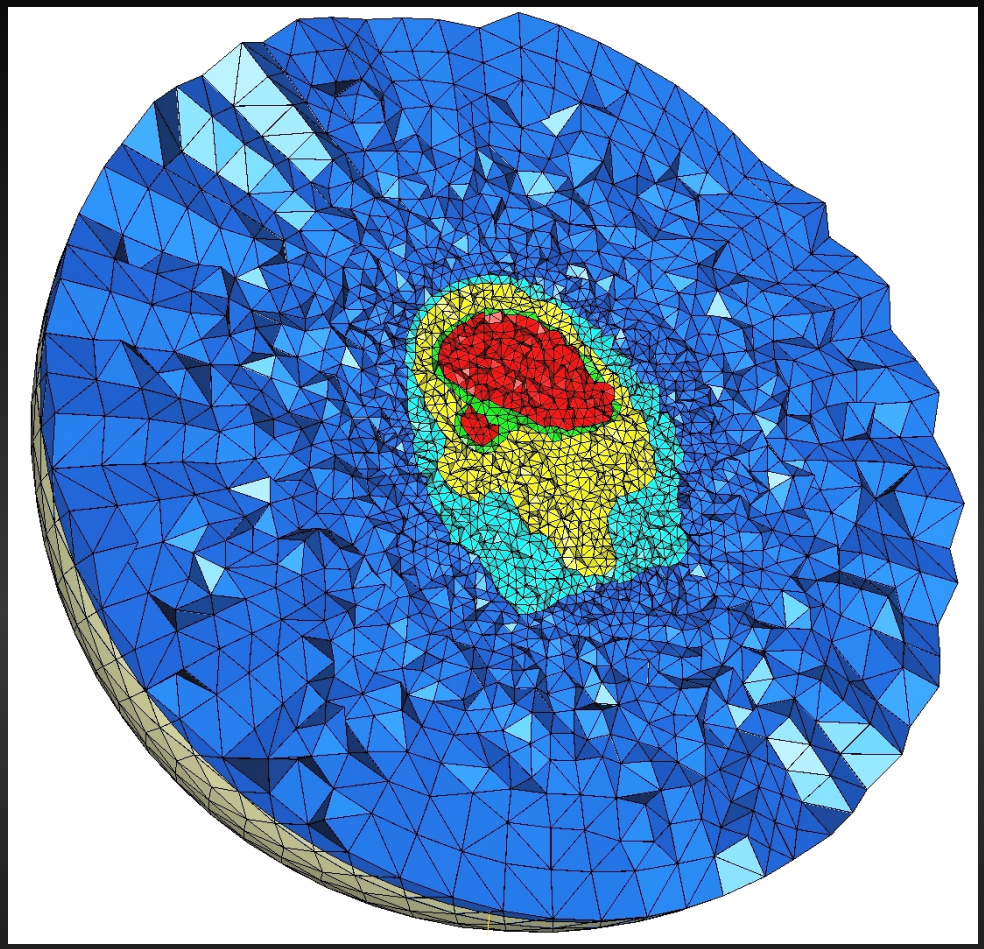

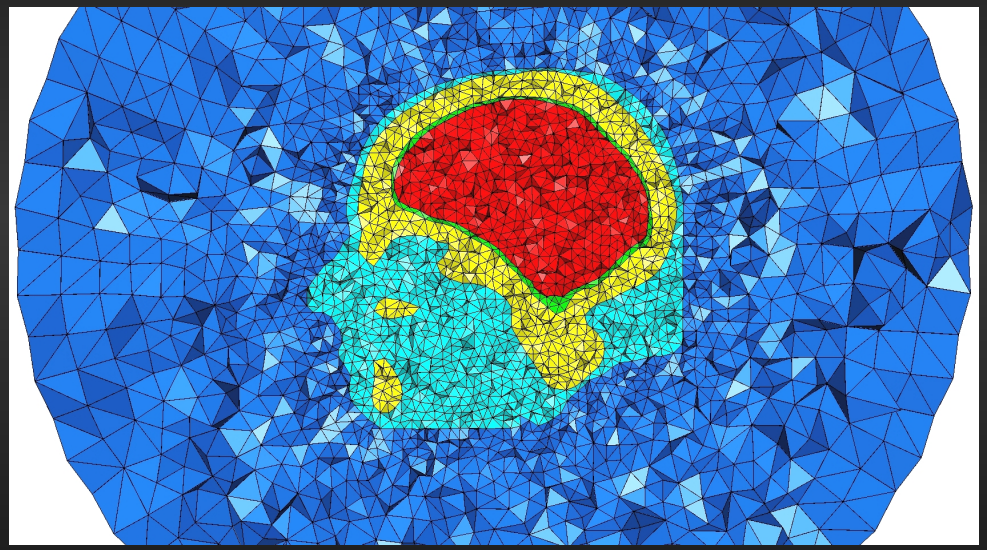

Tetrahedra : 361848

Hexahedra : 0

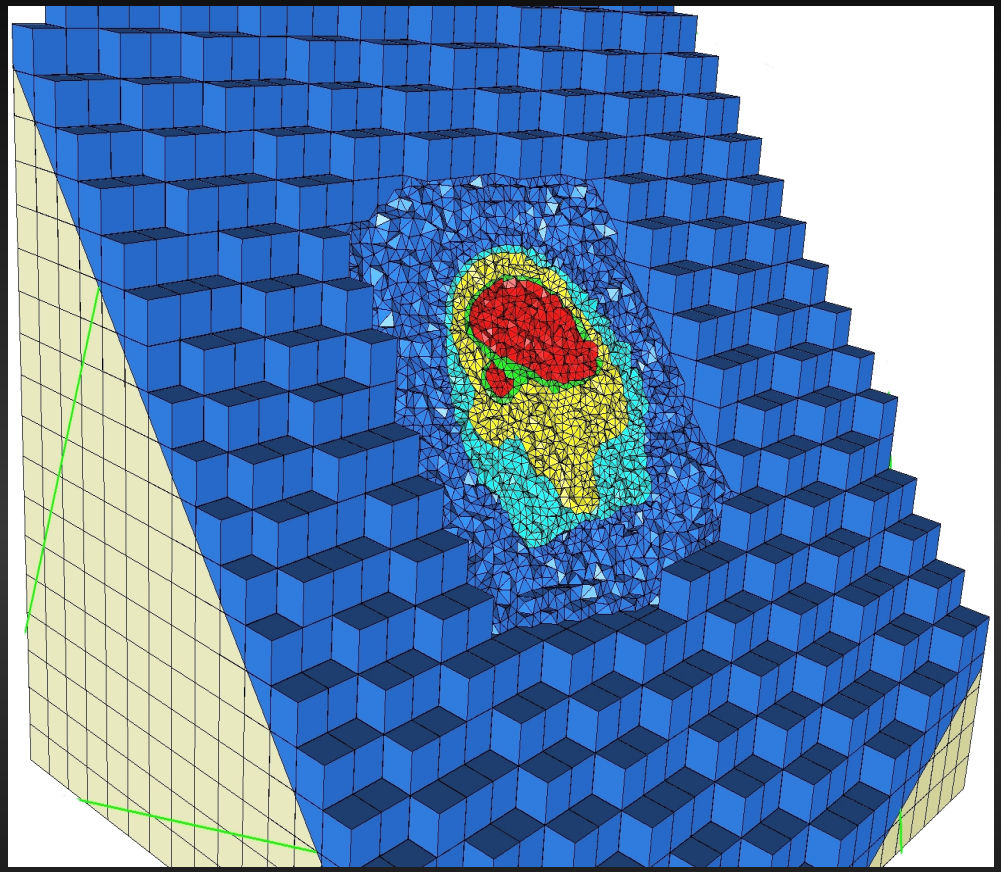

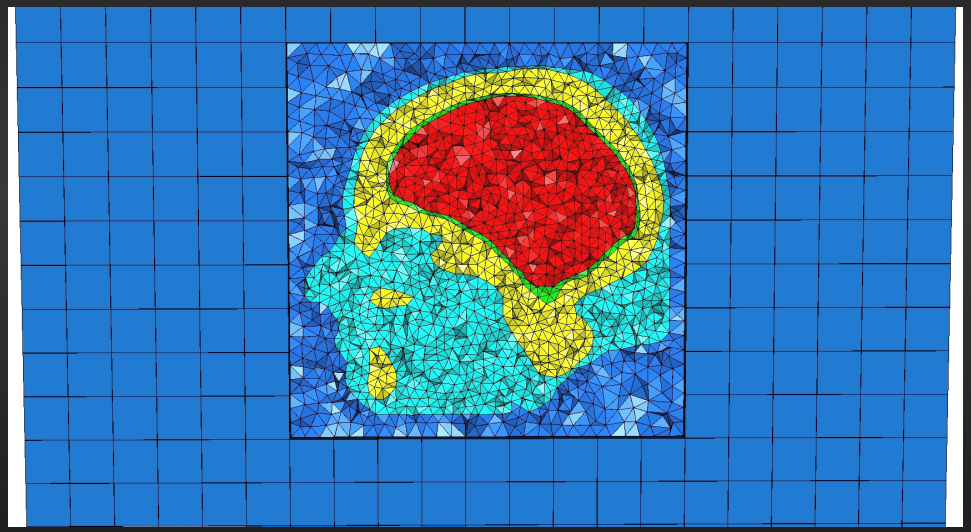

Tetrahedra : 288604

Hexahedra : 8532

- Spherical computational domain for the tetrahedral mesh : $R = 0.3$ m
- Cubic computational domain for the hybrid mesh : $[-0.3, 0.3]^3$
- Silver-Müller absorbing boundary condition
- Propagation of a wave emitted by a dipole type source, localized near to the right ear of the head. A current source term is imposed to the equation for the E_z component :

$$j_s^z(\mathbf{x}, t) = z_0 \ \delta(\mathbf{x} - \mathbf{x}^{cs}) \ \mathfrak{f}(t),$$

where z_0 is the wave impedance of the vacuum, δ is the zero-centered Dirac delta function, $\mathbf{x}^{cs}$ is the position of the source and the temporal signal $\mathfrak{f}(t)$ is a sinusoidal function. Finally, the frequency $f = 1.8$ GHz

Interpolation order	CPU time	# *dof*
DGTD-$\mathbb{P}_2$	4 h 55 min	3618480
DGTD-$\mathbb{P}_1\mathbb{Q}_2$	0 h 38 min	1384780
DGTD-$\mathbb{P}_2\mathbb{Q}_2$	3 h 0 min	3116404

- Spherical computational domain for the tetrahedral mesh : $R = 0.3$ m
- Cubic computational domain for the hybrid mesh : $[-0.3, 0.3]^3$
- Silver-Müller absorbing boundary condition
- Propagation of a wave emitted by a dipole type source, localized near to the right ear of the head. A current source term is imposed to the equation for the E_z component :

$$j_s^z(\mathbf{x}, t) = z_0 \ \delta(\mathbf{x} - \mathbf{x}^{cs}) \ \mathfrak{f}(t),$$

where z_0 is the wave impedance of the vacuum, δ is the zero-centered Dirac delta function, $\mathbf{x}^{cs}$ is the position of the source and the temporal signal $\mathfrak{f}(t)$ is a sinusoidal function. Finally, the frequency $f = 1.8$ GHz

Interpolation order	CPU time	# *dof*
DGTD-$\mathbb{P}_2$	4 h 55 min	3618480
DGTD-$\mathbb{P}_1\mathbb{Q}_2$	0 h 38 min	1384780
DGTD-$\mathbb{P}_2\mathbb{Q}_2$	3 h 0 min	3116404

- Spherical computational domain for the tetrahedral mesh : $R = 0.3$ m
- Cubic computational domain for the hybrid mesh : $[-0.3, 0.3]^3$
- Silver-Müller absorbing boundary condition
- Propagation of a wave emitted by a dipole type source, localized near to the right ear of the head. A current source term is imposed to the equation for the E_z component :

$$j_s^z(\mathbf{x}, t) = z_0 \ \delta(\mathbf{x} - \mathbf{x}^{cs}) \ \mathfrak{f}(t),$$

where z_0 is the wave impedance of the vacuum, δ is the zero-centered Dirac delta function, $\mathbf{x}^{cs}$ is the position of the source and the temporal signal $\mathfrak{f}(t)$ is a sinusoidal function. Finally, the frequency $f = 1.8$ GHz

Interpolation order	CPU time	# *dof*
DGTD-$\mathbb{P}_2$	4 h 55 min	3618480
DGTD-$\mathbb{P}_1\mathbb{Q}_2$	0 h 38 min	1384780
DGTD-$\mathbb{P}_2\mathbb{Q}_2$	3 h 0 min	3116404

Time evolution of H_y component at two points exterior to the head :

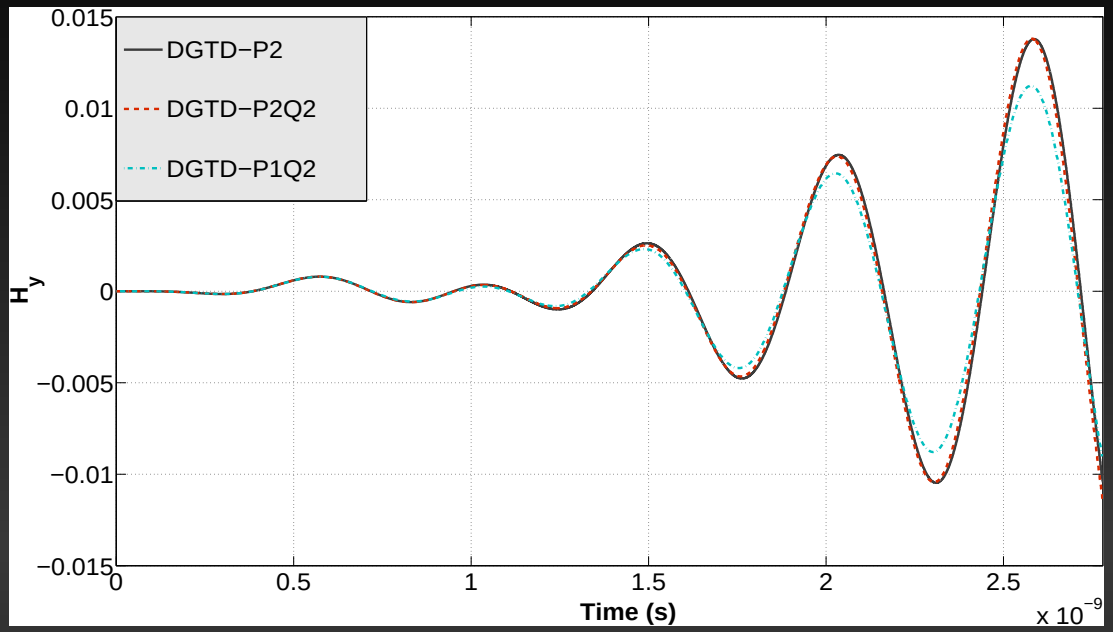

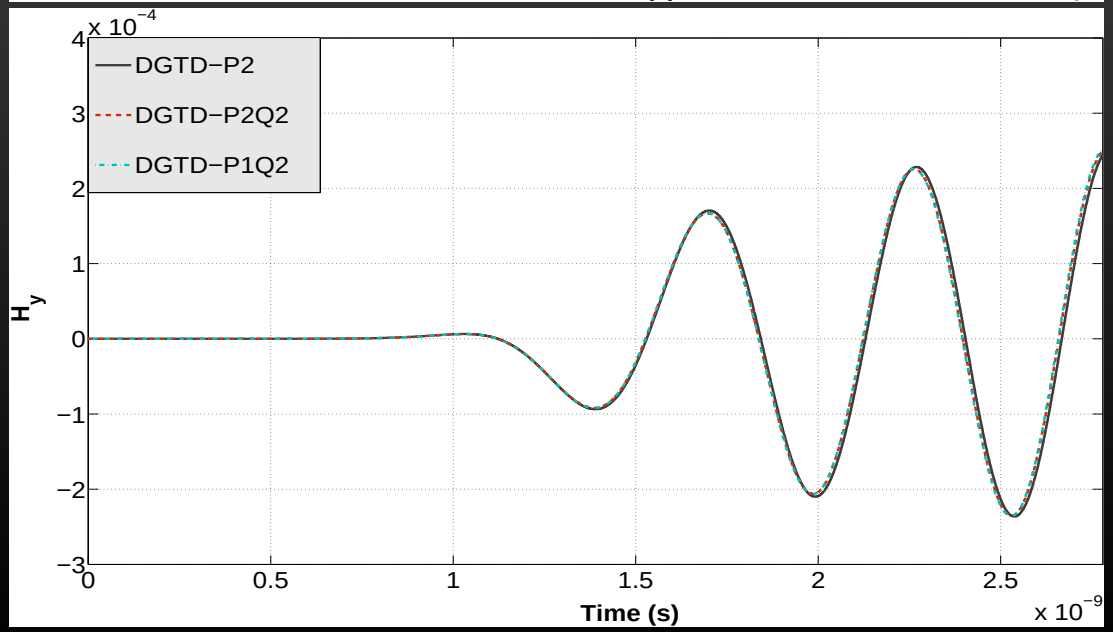

Time evolution of H_y component at two points interior to the head :

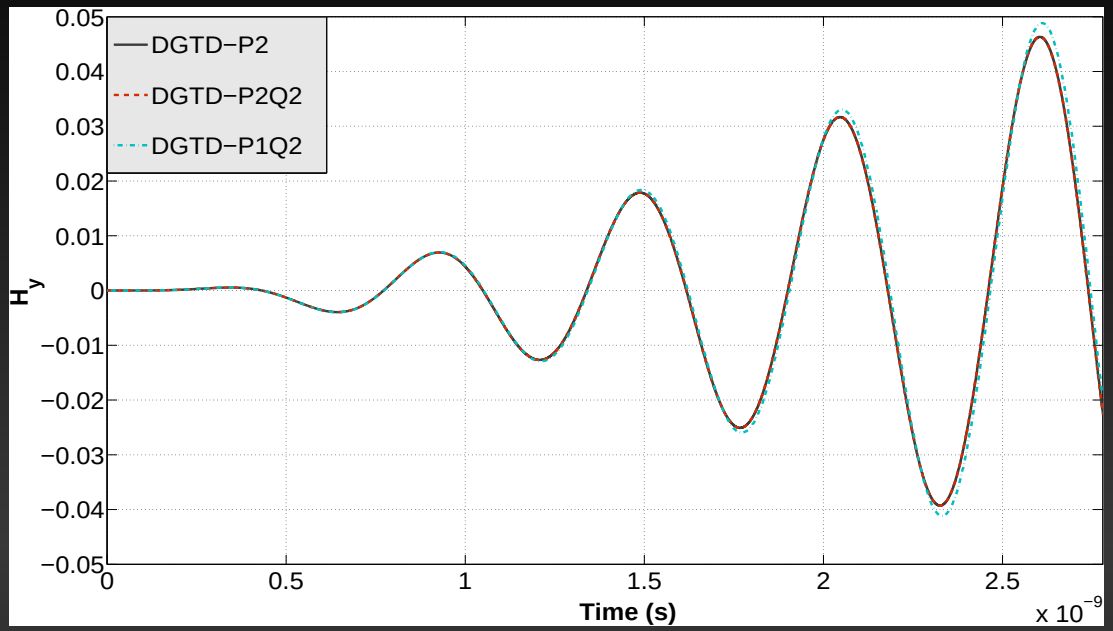

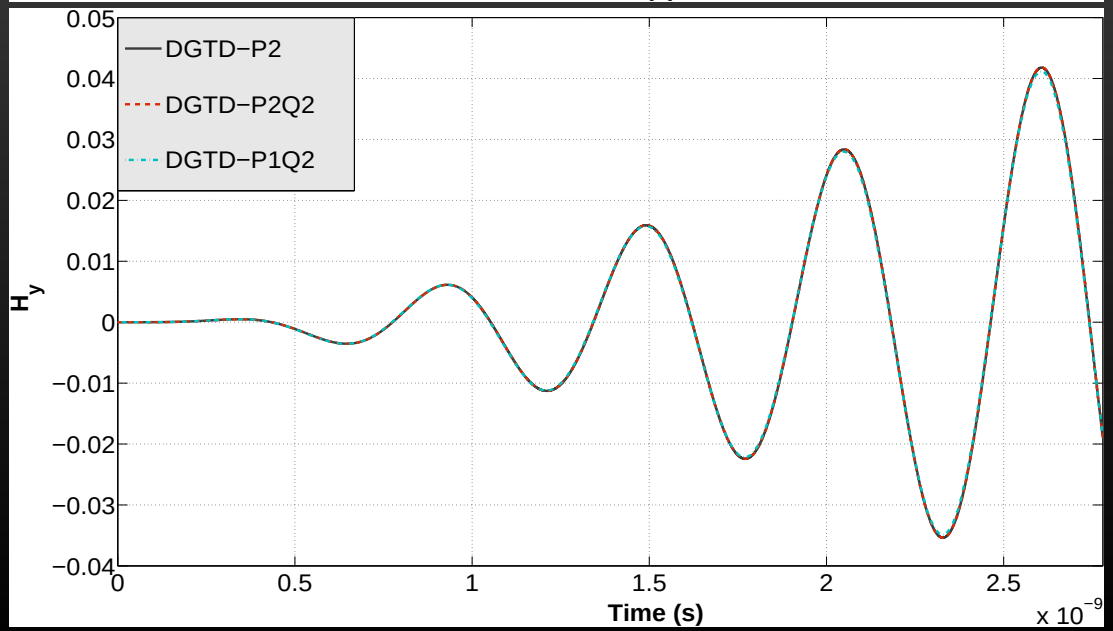

Contour lines of $\sqrt{E_{x,\text{four}}^2 + E_{y,\text{four}}^2 + E_{z,\text{four}}^2}$ for the DGTD-$\mathbb{P}_2$ method :

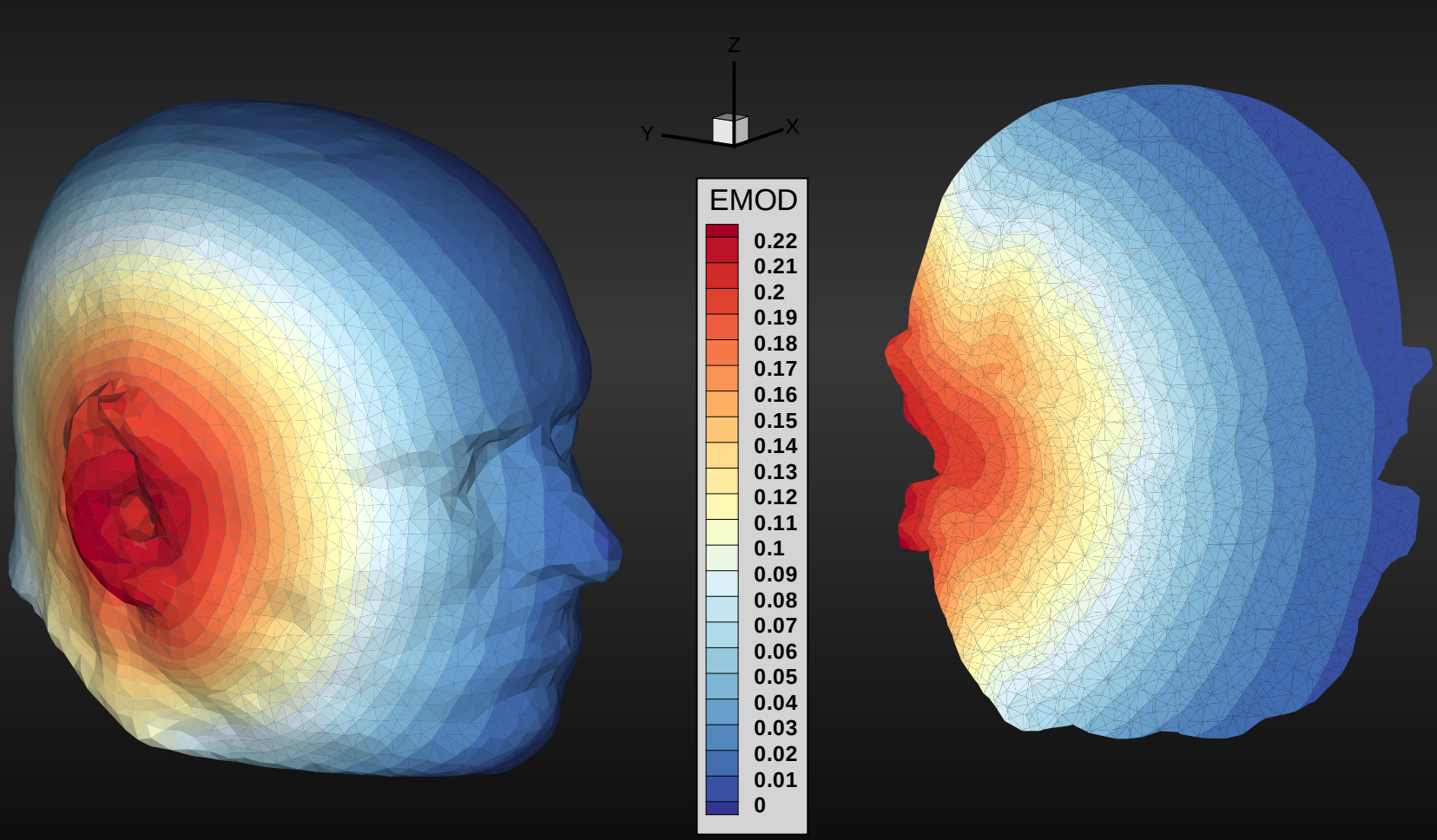

Contour lines of $\sqrt{E_{x,\text{four}}^2 + E_{y,\text{four}}^2 + E_{z,\text{four}}^2}$ for the DGTD-$\mathbb{P}_2\mathbb{Q}_2$ method :

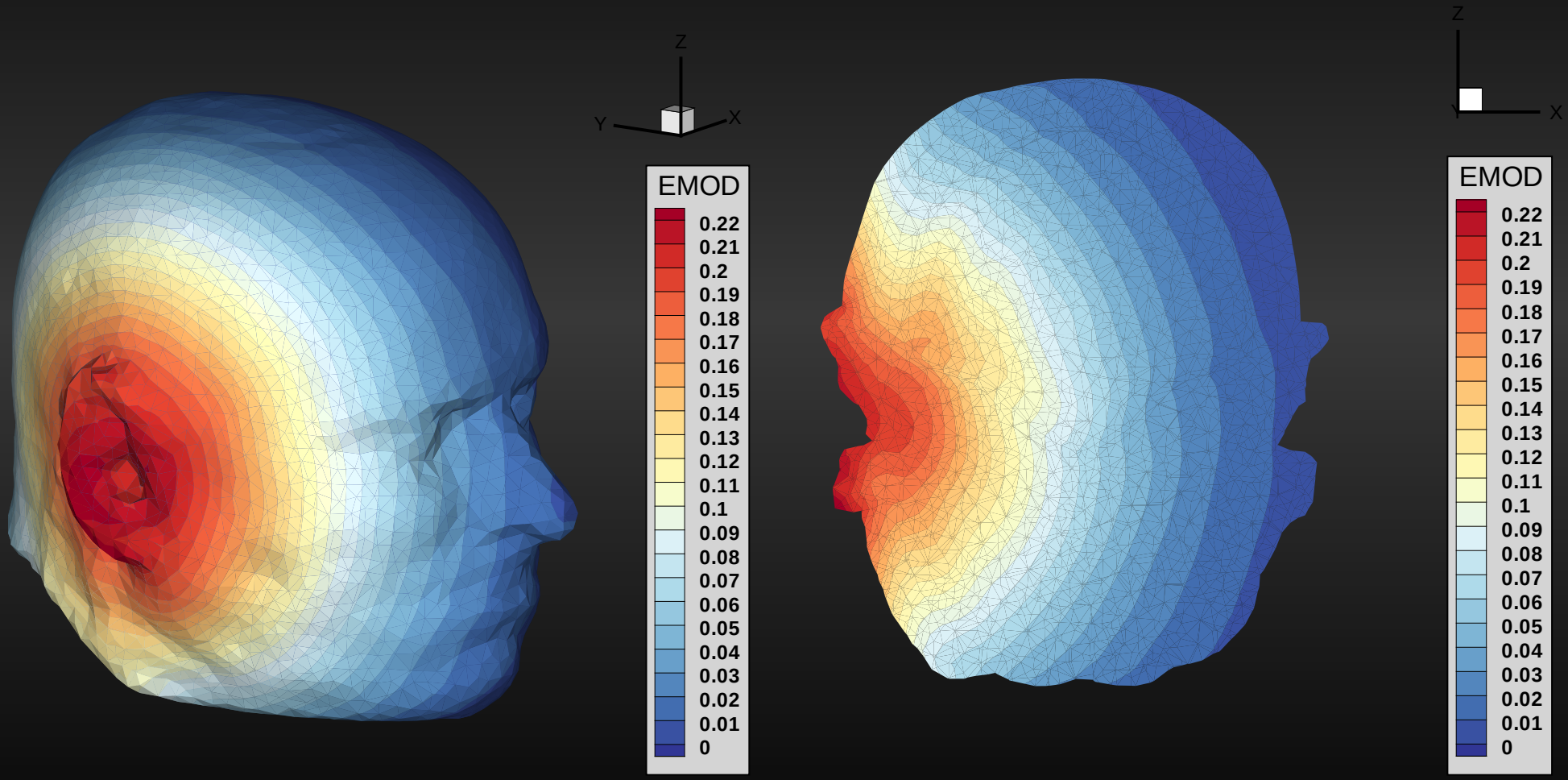

Contour lines of $\sqrt{E_{x,\text{four}}^2 + E_{y,\text{four}}^2 + E_{z,\text{four}}^2}$ for the DGTD-$\mathbb{P}_1\mathbb{Q}_2$ method :

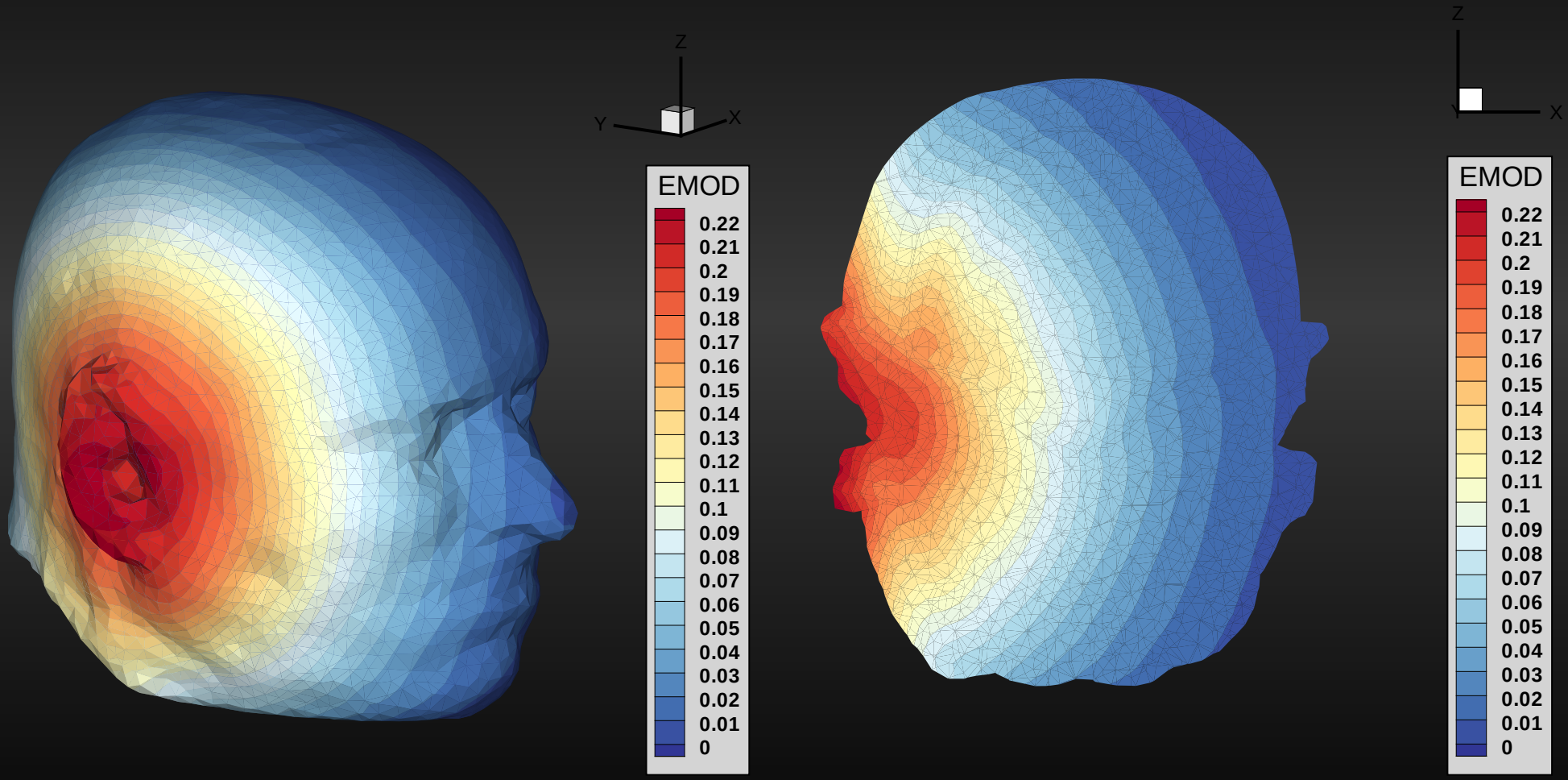

Outline

- Summarization :
  - Formulation of the DGTD-$\mathbb{P}_p\mathbb{Q}_k$ method on hybrid and non-conforming meshes
  - Validation, and consistency between the mathematical and numerical results
  - First ideas of efficiency improvements in 2D
  - Confirmation in 3D

- Future work :
  - Higher interpolation order and LF4 scheme for 3D numerical experiments, and parallel computing $\Longrightarrow$ Raphaël Léger postdoc
  - Using others basis function (orthogonal basis for $\mathbb{Q}_k$ on hexahedra)
  - Local explicit, or hybrid implicit/explicit time-stepping strategy $\Longrightarrow$ Ludovic Moya PhD thesis

    [17] L. Moya. *Temporal convergence of a locally implicit discontinuous Galerkin method for Maxwell's equations.* M2AN, vol. 46, no. 5, pp. 1225–1246, 2012.
  - Dispersive media $\Longrightarrow$ Jonathan Viquerat PhD thesis, and Claire Scheid

    [18] S. Lanteri and C. Scheid. *Convergence of a Discontinuous Galerkin scheme for the mixed time domain Maxwell's equations in dispersive media.* IMA Journal of Numerical Analysis, 2012.

- Summarization :
  - Formulation of the DGTD-$\mathbb{P}_p\mathbb{Q}_k$ method on hybrid and non-conforming meshes
  - Validation, and consistency between the mathematical and numerical results
  - First ideas of efficiency improvements in 2D
  - Confirmation in 3D

- Future work :
  - Higher interpolation order and LF4 scheme for 3D numerical experiments, and parallel computing $\Longrightarrow$ Raphaël Léger postdoc
  - Using others basis function (orthogonal basis for $\mathbb{Q}_k$ on hexahedra)
  - Local explicit, or hybrid implicit/explicit time-stepping strategy $\Longrightarrow$ Ludovic Moya PhD thesis

    [17] L. Moya. *Temporal convergence of a locally implicit discontinuous Galerkin method for Maxwell's equations.* M2AN, vol. 46, no. 5, pp. 1225–1246, 2012.
  - Dispersive media $\Longrightarrow$ Jonathan Viquerat PhD thesis, and Claire Scheid

    [18] S. Lanteri and C. Scheid. *Convergence of a Discontinuous Galerkin scheme for the mixed time domain Maxwell's equations in dispersive media.* IMA Journal of Numerical Analysis, 2012.

- Summarization :
  - Formulation of the DGTD-$\mathbb{P}_p\mathbb{Q}_k$ method on hybrid and non-conforming meshes
  - Validation, and consistency between the mathematical and numerical results
  - First ideas of efficiency improvements in 2D
  - Confirmation in 3D
- Future work :
  - Higher interpolation order and LF4 scheme for 3D numerical experiments, and parallel computing $\Longrightarrow$ Raphaël Léger postdoc
  - Using others basis function (orthogonal basis for $\mathbb{Q}_k$ on hexahedra)
  - Local explicit, or hybrid implicit/explicit time-stepping strategy $\Longrightarrow$ Ludovic Moya PhD thesis

    [17] L. Moya. *Temporal convergence of a locally implicit discontinuous Galerkin method for Maxwell's equations.* M2AN, vol. 46, no. 5, pp. 1225–1246, 2012.
  - Dispersive media $\Longrightarrow$ Jonathan Viquerat PhD thesis, and Claire Scheid

    [18] S. Lanteri and C. Scheid. *Convergence of a Discontinuous Galerkin scheme for the mixed time domain Maxwell's equations in dispersive media.* IMA Journal of Numerical Analysis, 2012.

Thank you for your attention